AD-A042667

AD

BRL MR

BRL

MEMORANDUM REPORT NO. 2761

(Supersedes IMR No. 474)

COUPLING OF X-RAY DEPOSITION TO STRUCTURAL RESPONSE

Henry L. Wisniewski

June 1977

Approved for public release; distribution unlimited.

USA ARMAMENT RESEARCH AND DEVELOPMENT COMMAND
USA BALLISTIC RESEARCH LABORATORY
ABERDEEN PROVING GROUND, MARYLAND

UNCLASSIFIED

SECURITY CLASSIFICATION OF THIS PAGE (When Data Entered)

REPORT DOCUMENTATION PAGE

READ INSTRUCTIONS BEFORE COMPLETING FORM

1. REPORT NUMBER: BRL MEMORANDUM REPORT NO. 2761
2. GOVT ACCESSION NO.:
3. RECIPIENT'S CATALOG NUMBER:
4. TITLE (and Subtitle): COUPLING OF X-RAY DEPOSITION TO STRUCTURAL RESPONSE
5. TYPE OF REPORT & PERIOD COVERED: Final
6. PERFORMING ORG. REPORT NUMBER:
7. AUTHOR(s): Henry L. Wisniewski
8. CONTRACT OR GRANT NUMBER(s):
9. PERFORMING ORGANIZATION NAME AND ADDRESS: USA Ballistic Research Laboratory, Aberdeen Proving Ground, Maryland 21005
10. PROGRAM ELEMENT, PROJECT, TASK AREA & WORK UNIT NUMBERS: RDT&E 1W162118AH75
11. CONTROLLING OFFICE NAME AND ADDRESS: US Army Materiel Development and Readiness Command, 5001 Eisenhower Avenue, Alexandria, VA 22333
12. REPORT DATE: JUNE 1977
13. NUMBER OF PAGES: 78
14. MONITORING AGENCY NAME & ADDRESS (if different from Controlling Office):
15. SECURITY CLASS. (of this report): UNCLASSIFIED
15a. DECLASSIFICATION/DOWNGRADING SCHEDULE:
16. DISTRIBUTION STATEMENT (of this Report): Approved for public release; distribution unlimited.
17. DISTRIBUTION STATEMENT (of the abstract entered in Block 20, if different from Report):
18. SUPPLEMENTARY NOTES: Supersedes BRL Interim Memorandum Report No. 474.
19. KEY WORDS (Continue on reverse side if necessary and identify by block number):
X-Ray Loading
Blow-off
Structural Response
Finite-Difference
Flat Plate
Spall

20. ABSTRACT (Continue on reverse side if necessary and identify by block number) (bas)

The need for a reliable and efficient method to predict the structural response of target structures to x-ray loading prompted the coupling of the x-ray deposition program, RIP, to the structural response program, PETROS 3. The RIP program predicts that material on the front face will blow-off as liquid-solid, liquid and vapor, thus delivering an impulsive load. Simultaneously a stress wave is transmitted through the residual solid material causing spallation on the back face. (Continued)

DD FORM 1473, 1 JAN 73 — EDITION OF 1 NOV 65 IS OBSOLETE

UNCLASSIFIED

SECURITY CLASSIFICATION OF THIS PAGE (When Data Entered)

Item 20 - Continued

The RIP program was modified to provide specific output characteristics of the residual solid material namely: thickness, mean transverse velocity, and through-thickness distribution of temperature and tangential stresses which remain after the transverse elastoplastic stress waves have dissipated. The BRL version of PETROS 3 program was then modified to accept these data as initial conditions.

A structural response test case was treated using both undegraded and degraded material properties, the solutions of which show a large disparity in output results.

TABLE OF CONTENTS

LIST OF ILLUSTRATIONS

LIST OF TABLES

I. INTRODUCTION

The principal kill mechanism of target structures in an exoatmospheric nuclear environment is most likely to be x-ray deposition and the accompanying material response due to heating. The various material responses can consist of melting, vaporization, shock wave propagation, and spallation.

The physical phenomenology of the material response involved can be related as follows. Initially the external surface (front face), assuming slab geometry, is heated almost instantaneously to high temperatures causing material to melt and blow-off in the form of vapor, liquid-vapor, liquid, or solid-liquid. The impulsive load due to the blow-off creates a stress wave that propagates into the interior of the target toward the bottom surface (back face). Simultaneously the material below the top surface is heated, inducing a compressive stress which propagates to the bottom surface (back face) and reflects as a rarefaction tensile stress wave. At some point near the bottom surface this rarefaction tensile stress wave overpowers the compressive stress wave moving toward the bottom surface, and the high tension produced may cause spalling.

The consequence of the material response is that it leaves the target in a weakened condition. In order to have a capability to predict damage to the structure, RIP[1, 2, 3, 4] was coupled to PETROS 3[5]. The coupling was done on the premise that calculations of material response (which normally cover a period of a few microseconds, at most) and predictions of structural response (which generally involve response durations on the order of milliseconds) can be performed consecutively rather than requiring a simultaneous treatment.

---

[1] *R. H. Fisher, G. A. Lane, and R. A. Cecil, "RIP, A One-Dimensional Material Response Code - User's Guide," Systems, Science and Software, Report 3SR-751-I, September 1972.*

[2] *R. H. Fisher, G. A. Lane, and R. A. Cecil, "RIP, A One-Dimensional Material Response Code - Code Reference Manual," Systems, Science and Software, Report 3SR-751-II, September 1972.*

[3] *R. A. Kruger, "The Material Response Program, RIP," Systems, Science and Software, Report 3SR-120, December 1969.*

[4] *RIP, A One-Dimensional Material Response Code. Systems, Science and Software, Contract No. SSS-R-72-1324.*

[5] *S. Atluri, E. A. Witmer, J. W. Leech, and L. Morino, "PETROS 3: A Finite Difference Method and Program for the Calculation of Large Elastic-Plastic Dynamically Induced Deformations of Multilayer Variable - Thickness Shells," U.S. Army Ballistic Research Laboratories, Contract Report No. 60, November 1971 (AD #890200L).*

This report presents the calculational procedure used to predict the structural response of a 6061-T6 aluminum flat plate. The input and results of RIP calculations are presented along with a comparison of two structural response calculations utilizing PETROS 3.

Appendix A contains the code modifications required in the RIP code to permit the appropriate data to be extracted for use as input to the PETROS 3 structural response calculations. In order to expedite analysis of structural response output data, a plotting program was developed. A description of this program is presented in Appendix B along with a listing. The BRL version of PETROS 3 required some minimal modifications and these are described in Appendix C. Appendix D contains temperature variation data related to temperature changes which occurred during the structural response calculations.

II. CALCULATIONAL PROCEDURE

A physical description of the problem is portrayed diagrammatically in Figure 1. The target is a flat rectangular plate which is partitioned into numerous rectangular columns of material made up of smaller volumes of material called mass zones. The purpose of this geometry is the accommodation of the fact that the RIP code is one-dimensional. Thus for the RIP calculations, it is sufficient to concentrate on a specific column. As Figure 1 indicates, the x-rays impinge on the top mass zone of the column thus depositing energy and consequently heating the material to high temperatures. A stress wave is generated and the situation shown in Figure 1 develops. Some of the material is removed from the front face as liquid, liquid-solid, vapor and vapor-liquid (for this work, only a phase change to liquid and liquid-solid takes place). Stress waves in the solid material caused both by this material removal and by non-uniform heating, after reflection from the bottom surface (free-boundary), resulted in sufficiently large tensile stress to cause spallation.

The RIP code employs a Lagrangian finite difference method and computes the material response due to rapid heating by solving simultaneously the equations of conservation of mass, momentum, and energy.

The Gray* equation of state was used in conjunction with the simple von Mises elastic-plastic model, in which the yield behavior is calculated from the shear modulus and yield strength. An energy dependent peak tensile strength spall model was used where the spall strength is a function of the melt energy. If the energy is greater than the melt

---

***The Gray equation of state was chosen because temperature is computed directly. If any other equation of state options provided by RIP were used, additional calculations would have to be added.*

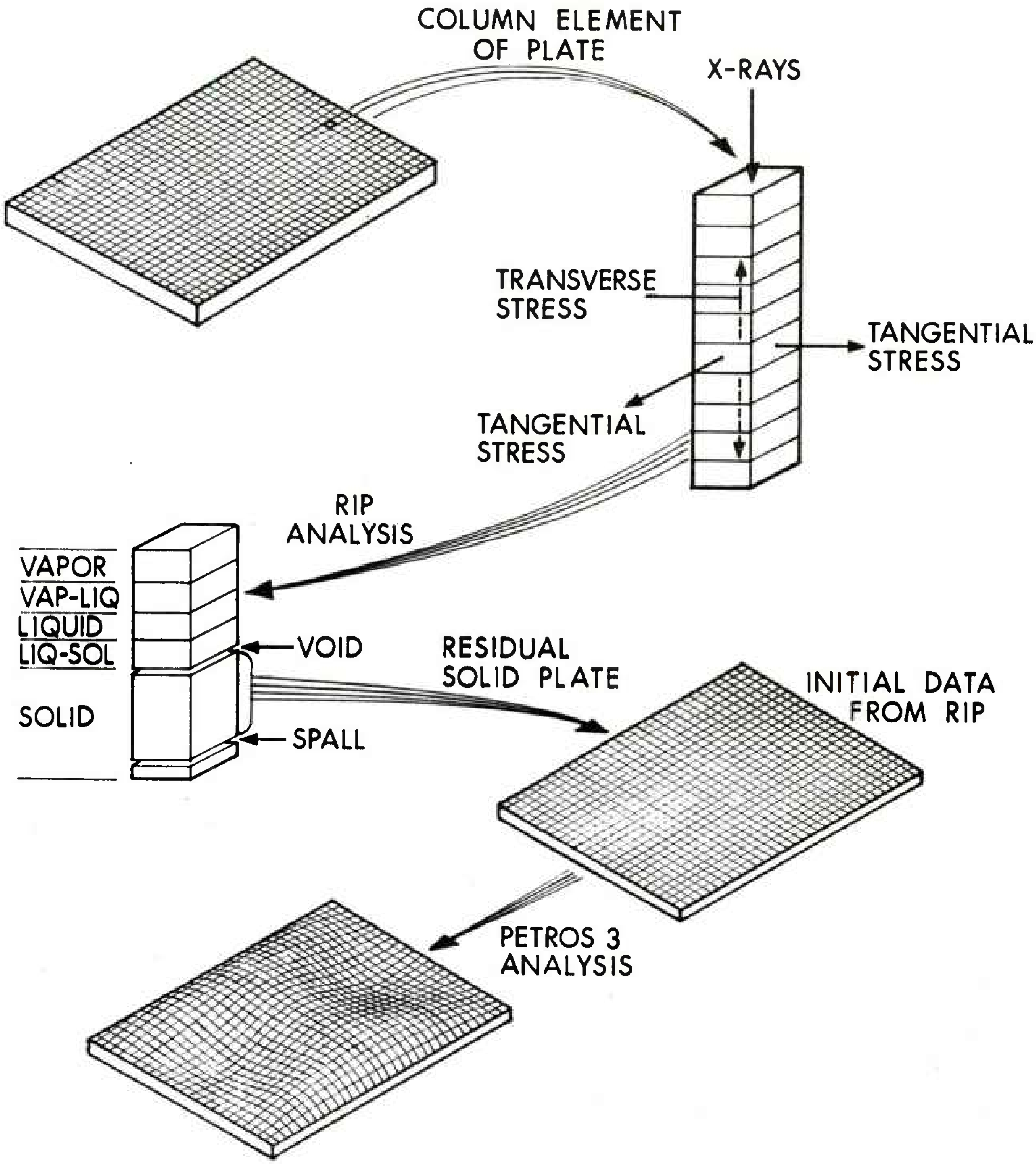

Figure 1. Representation of the Coupling between RIP and PETROS 3

energy, the material is assumed to have zero strength and spallation will be initiated. If the energy is less than the melt energy, the tensile stress level required to initiate spallation is assumed to be the value of the spall strength.

The coupling was performed by running the RIP program as shown in Figure 2, from $t_R = 0$, with an x-ray radiation source of 10 kev blackbody spectrum, a fluence level of 80 cal/cm^{2}* and a shine time of 75 nanoseconds, to a termination time, t_{RF}. This time is determined by a damping model described in Reference 6, page 46. This damping model requires that each piece of solid material be brought to a uniform velocity, rather than to a static equilibrium. It was incorporated in RIP so that after

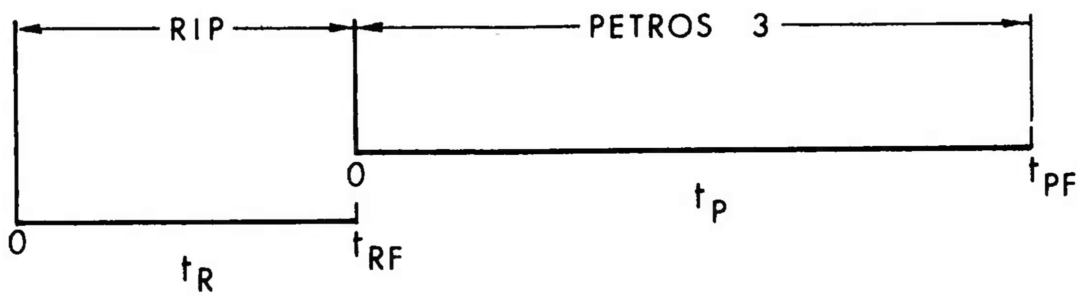

Figure 2. Time History of the Coupling

considerable time transverse (through-thickness) wave motion would vanish throughout the solid material leaving the residual material and each spall fragment with individual uniform velocity. The damping can be activated at any specified time step after the plastic work and spallation are essentially complete. This determination was arrived at by analyzing the results of a run without damping as explained in Section III of this report.

A fluence level of 80 cal/cm^2 was selected in order to guarantee blowoff on the front face and spallation on the backface.

[6] *J. M. Santiago, H. L. Wisniewski, N. J. Huffington, Jr., "A User's Manual for the REPSIL Code," U.S. Army Ballistic Research Laboratories, Report No. 1744, October 1974. (AD #A003176)*

At RIP termination time, t_{RF}, the largest residual solid and its physical data, thickness, mean transverse velocity, through-thickness distribution of temperature and tangential stresses are transferred to a rectangular flat plate to serve as initial conditions to the BRL version of PETROS 3 calculations as shown in Figure 1.

PETROS 3 also uses a finite difference method. It solves the partial differential equations of motion that govern large deflections and elastic-plastic (von Mises model, consistent with RIP calculations) behavior of thin Kirchhoff shells exposed to impulsive/pressure loadings.

In working with the RIP program, it was found that the equation of state, (Gray EOS), performs the calculation as if the material were rapidly heated, while the elastic-plastic (von Mises model) calculation is carried out as if the material is cold (room temperature) or at least values of elastic modulus and yield stress remain constant. The basis for this assumption is that for the short time period covered by the RIP calculation, there is insufficient time for thermal degradation of material properties. Proof of this remains to be established for material which has been heated nearly to its melting point. However, due to this inconsistency in RIP between the equation of state and the elastic-plastic calculation it was felt worthwhile to attempt to bracket the true response by performing two PETROS 3 calculations using (a) undegraded material parameters (results labeled cold material properties) and (b) material properties associated with long soak times at elevated temperatures (results labeled hot material properties).

At time $t_p = 0$, the PETROS 3 program reads in the geometry of the plate and the physical data of the material from the RIP solution. Mean transverse velocity is uniform for every finite difference mesh point in the Y^1, Y^2 plane (see Figure 3). In the Y^3 direction, the thickness, which is uniform for the plate, is divided into a number of discrete layers at each mesh point.

Values of tangential stress and temperature* are constant for each layer in the Y^1, Y^2 plane, but vary for each layer. The number and thickness of the layers depend on the number of points one wishes to use with the Gaussian integration in determining force and moment resultants.

**The temperature distribution throughout the structural response solution remains constant. A discussion of this point is presented in Appendix C.*

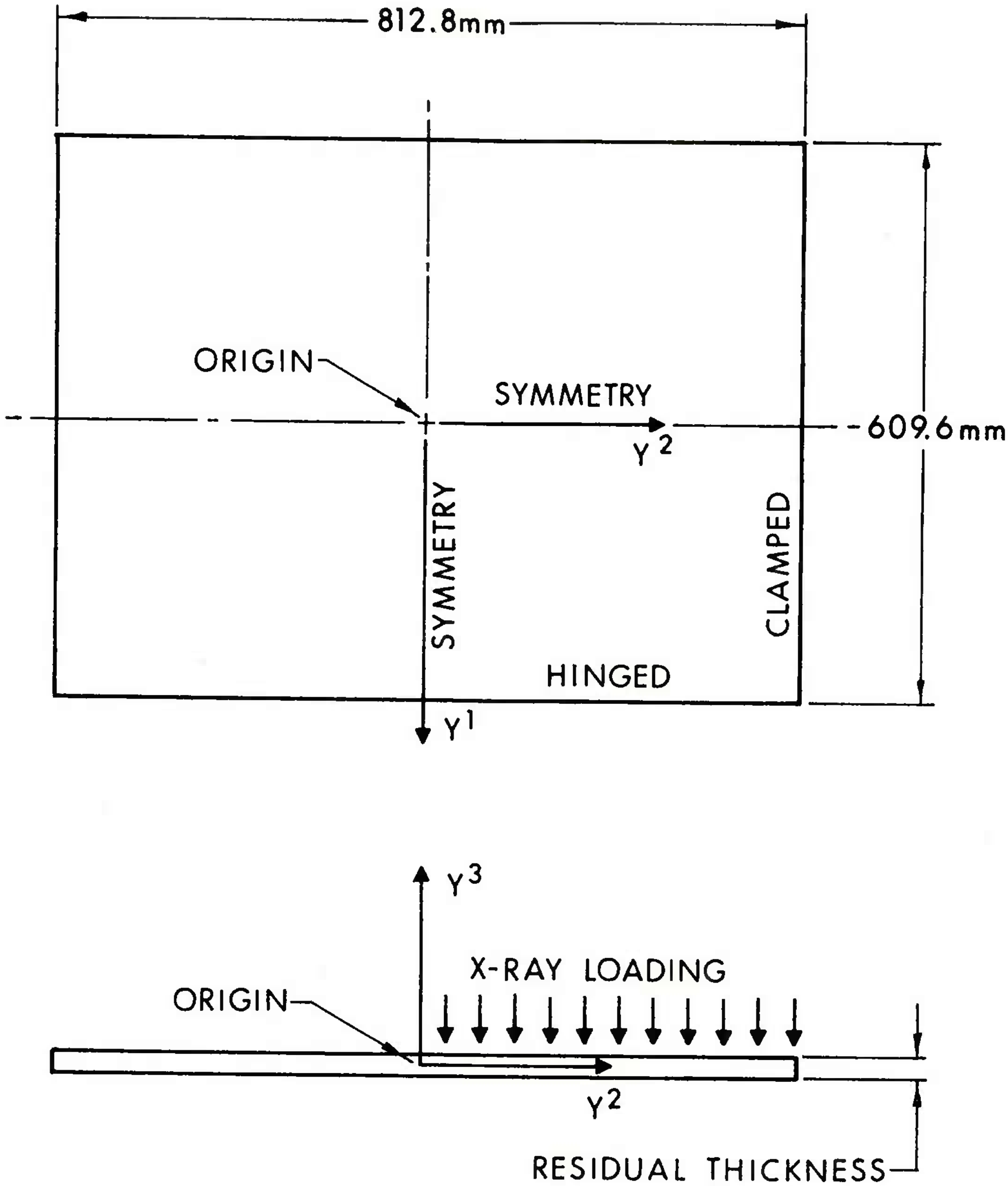

Figure 3. Flat Plate Geometry (6061-T6 Aluminum)

III. RIP INPUT AND RESULTS

The input cards listed in Table I are the input parameters required to perform the RIP calculation. They are defined in Reference 1, pages 3 through 33. The parameters for the Gray equation of state subroutine are listed in Table II.

Figure 4 shows the energy per gm (dose) deposited through the initial thickness (5 mm) which was computed by the energy deposition and transport program FSCATT[7, 8]. This program serves as the x-ray radiation source for RIP. Figure 5 shows a representation of the column element of material at the end of the RIP calculation. It has gone through various phase changes due to x-ray energy deposition. The loss of material due to blowoff on the front-face is in the form of liquid and liquid-solid material, while the loss of material on the back-face is caused by spallation in the solid region.

The RIP code calculates the hydrostatic pressure P and the deviatoric stress, SD, (which is actually the component of deviatoric stress, σ_3', associated with the through-thickness direction). The transverse (through-thickness) stress, σ_3, (see Figure 5) is given* by $\sigma_3 = \sigma_3' + P$. In order to determine residual stresses, the RIP code has been modified to provide for damping out the transverse stress waves. Figure 6 shows the distribution of transverse stresses at t_{RF}. It may be seen that these stresses are negligible throughout the thickness of the solid material. However, the corresponding hydrostatic pressures shown in Figure 7 are non-negligible.

Since we know that the sum of the deviatoric stress components must vanish and that the tangential stresses, σ_1, σ_2, must be equal for the one-dimensional RIP analysis, it follows that $\sigma_1 = \sigma_2 = P - \frac{1}{2}$ SD, as plotted in Figure 8. It should be noted that, for the σ_3 stresses fully damped out, $\sigma_1 = \sigma_2 = 1.5$ P. These tangential stresses are the combined result of the inelastic deformation produced by the transverse stress waves and the thermal stresses corresponding to the temperature distribution at t_{RF} (see Figure 9).

---

[7] *R. H. Fisher and J. W. Wiehe, "A User's Guide to the FSCATT Code," Systems, Science and Software, Report 3SR-318, November 1970.*

[8] *R. H. Fisher and R. A. Kruger, "A Numerical Treatment of Scattering and Fluorescence in Plane Geometry," Systems, Science and Software, Report 3SR-119, September 1969.*

* *For the RIP analysis, compressive stresses are considered positive.*

Table I. Input for RIP Calculation

```
(AMASS)            B1=1.352
(MATBND)           B31=100
(MATLID)           B41=103
(NMTRLS)           B61=1
(MAXCYCL)          B84=995
(MODE)             B85=0
(TMAX)             B87=6.0E-04
(IOUNIT)           B245=2*-1,3*0,4
(NABS)             B291=1,17
(NORD)             B296=18,11
(NDUMP)            B313=1000
(NPRINT)           B315=100
(TPRINT)           B316=1.92396E-06
(DISCPT)           B1329=12A
        X-RAY LOADING ON 6061-T6 ALUMINUM
(ICOMBZ)                X1051=1
(SPALL CRITERIA)        X1052=1
(NSPALL)                X1001=3
(BBTEMP)           B182=10.0
(ENERGY1)          B185=-80.0
(SSTART1)          B219=0.
(SSTOP1)           B221=.75E-07
(NFIT)             B227=1
(GEOSAL)           V661=2.704,0.,0.,0.,0.,5.21E5,2.75162E11,2.69948E9,
                        -1.3E10,1.2E11,3.05E10,1.1E10,7.15E9,0.,0.,
                        1.338,2.18,1.68,.666667,8.7E-9,1340.,0.,0.,26.98,
                        .452,.190,47.,1.,11.4696E-5,3.
(END OF DATA)           END
    1  400    }
    1         }  See Appendix A for detailed explanation.
 1.           }
 1.80E-06     10.0 }
BBODYX             -1
0
                   1       14     .006
                   1       12     .01
                   1       29     .0025
                   1       24     .002
1                  1       13     .9795
```

Table II. Gray Equation of State Parameters for 6061-T6 Aluminum

Symbol	Numerical Value		Property
ρ_o	2.704	gm/cm^3	Ambient density[9]
C_o	5.21×10^5	cm/sec	Bulk sound speed[9]
AMU	2.751×10^{11}	$dynes/cm^2$	Shear Modulus[9]
Y_o	2.699×10^9	$dynes/cm^2$	Yield strength[9]
σ_o	-1.3×10^{10}	$dynes/cm^2$	Spall limit[1]
E_{VV}	1.2×10^{11}	ergs/cm	Material has vaporized[1]
E_{LV}	3.05×10^{10}	ergs/cm	Material commences to vaporize[1]
E_{LM}	1.10×10^{10}	ergs/cm	Material has completed melting[1]
E_{SM}	7.15×10^9	ergs/cm	Material commences to melt[1]
S	1.338		Hugoniot parameter[12]
γ_o	2.18	dimensionless	Lattice gamma[12]
a	1.68		$a = \gamma_o - .5$[12]
γ_e	.6667		Electronic gamma[11]
g_e	8.7×10^{-9}	Mbar cm^3/mole deg^2	Electronic energy coefficient[10]
T_{mo}	1340.	^oK	Melting temperature parameter[12]
E_{OH}	0.	Mbar cm^2/gm	Energy at reference state[12]
AW	26.98	gm/mole	Atomic weight[10]
V_J	.452	cm^3/gm	Volume at which EOS are joined[12]
V_b	.190	cm^3/gm	Excluded volume for vapor phase[12]
a_y	47.	Mbar (cm^3/mole)	Coefficient of attractive potential for vapor[12]
θ	1.0	dimensionless	Join parameter[12]
DELS	11.469×10^{-4}	Mbar cm^3/mole deg	Entropy of melting[12]

[9] *B. J. Kohn, "Compilation of Hugoniot Equations of State," Air Force Weapons Laboratory, April 1969 (page 19).*

[10] *Sensitivity of Material Response Calculations to the Equation of State Model, Systems, Science and Software, Contract Report No. 130 (SSS-R-73-1910), December 1973 (page 24).*

[11] *E. B. Royce, "Gray, A Three-Phase Equation of State for Metals," Lawrence Livermore Laboratory, Report UCRL-51121, September 1971 (page 38).*

[12] *R. B. Oswald, Jr., F. B. McLean, D. R. Schallhorn, and T. R. Oldham, "The Dynamic Response of Aluminum to Pulsed Energy Deposition in the Melt-Dominated Regime," U.S. Harry Diamond Laboratories, HDL-TR-1624, July 1973 (page 11).*

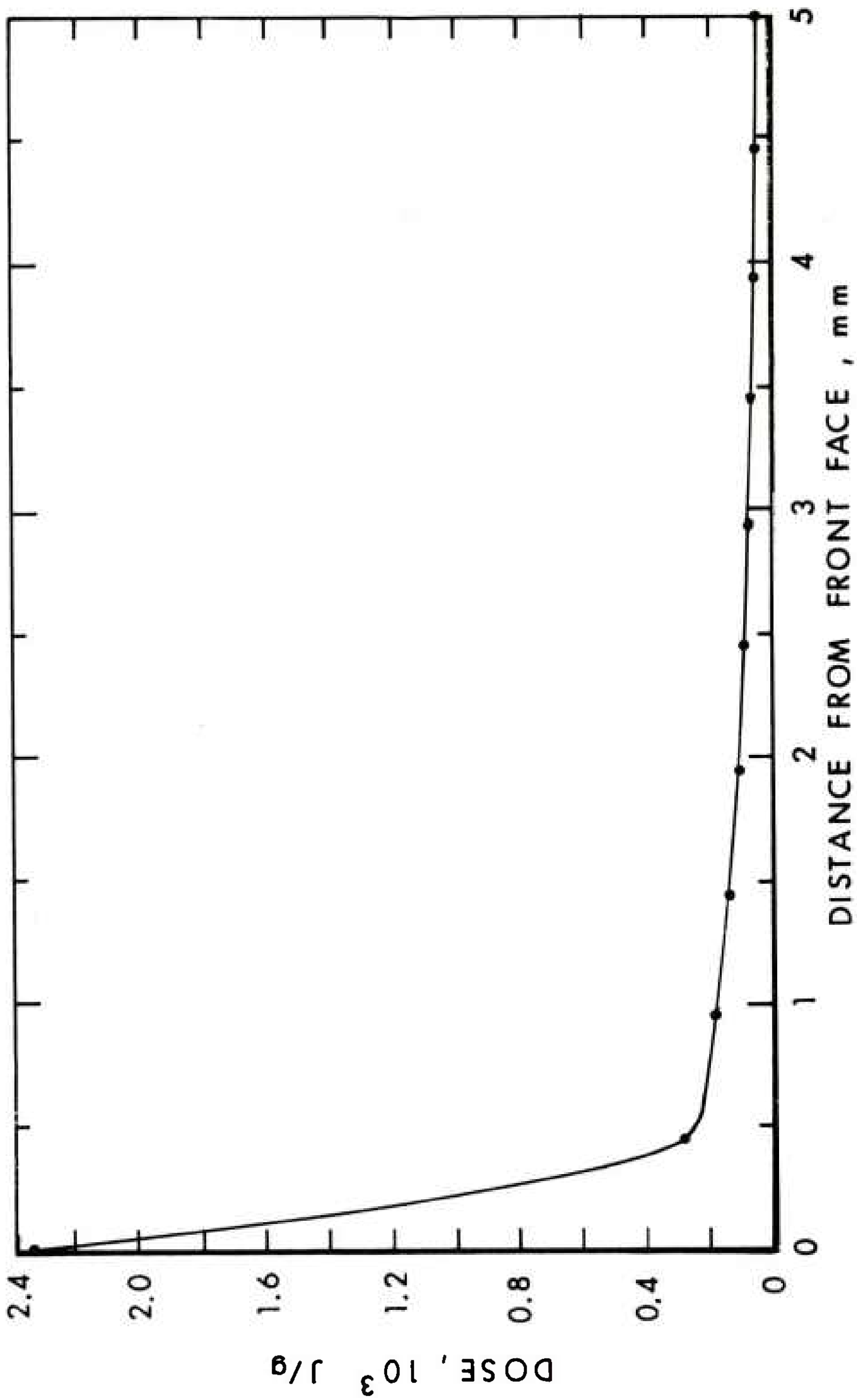

Figure 4. 10 Kev Blackbody Dose Profile

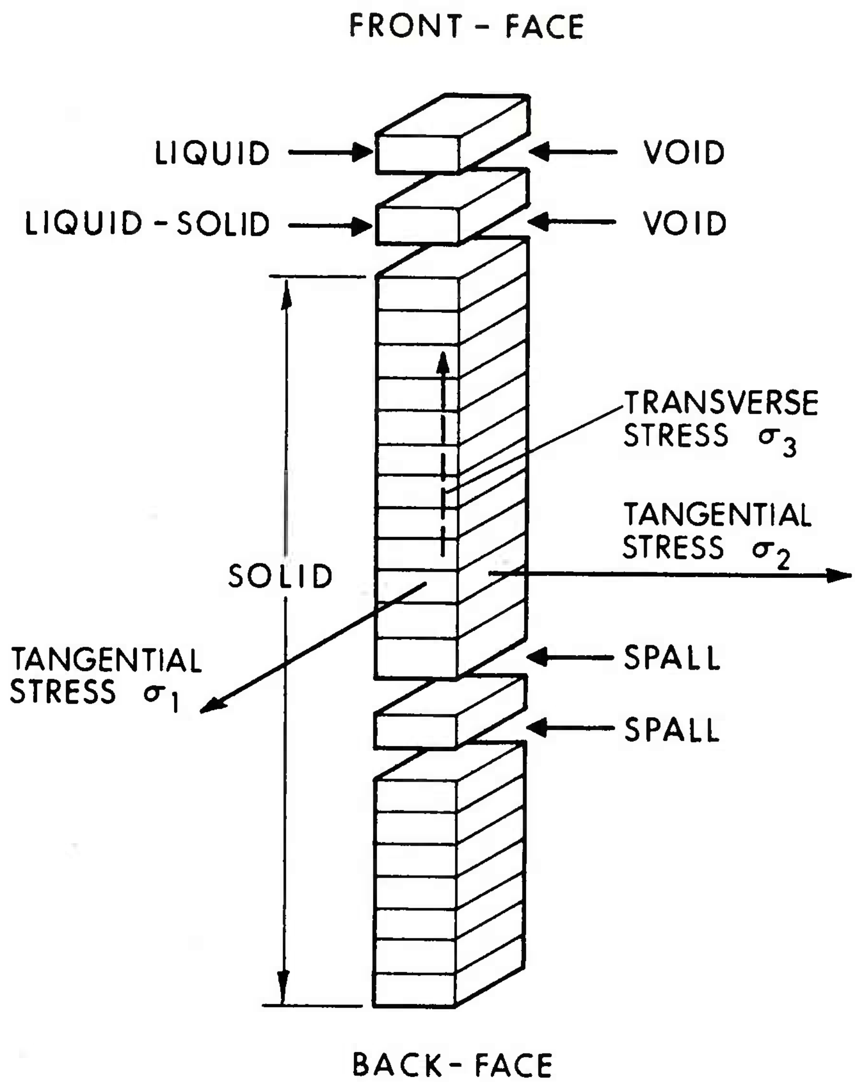

Figure 5. Material Break-Up

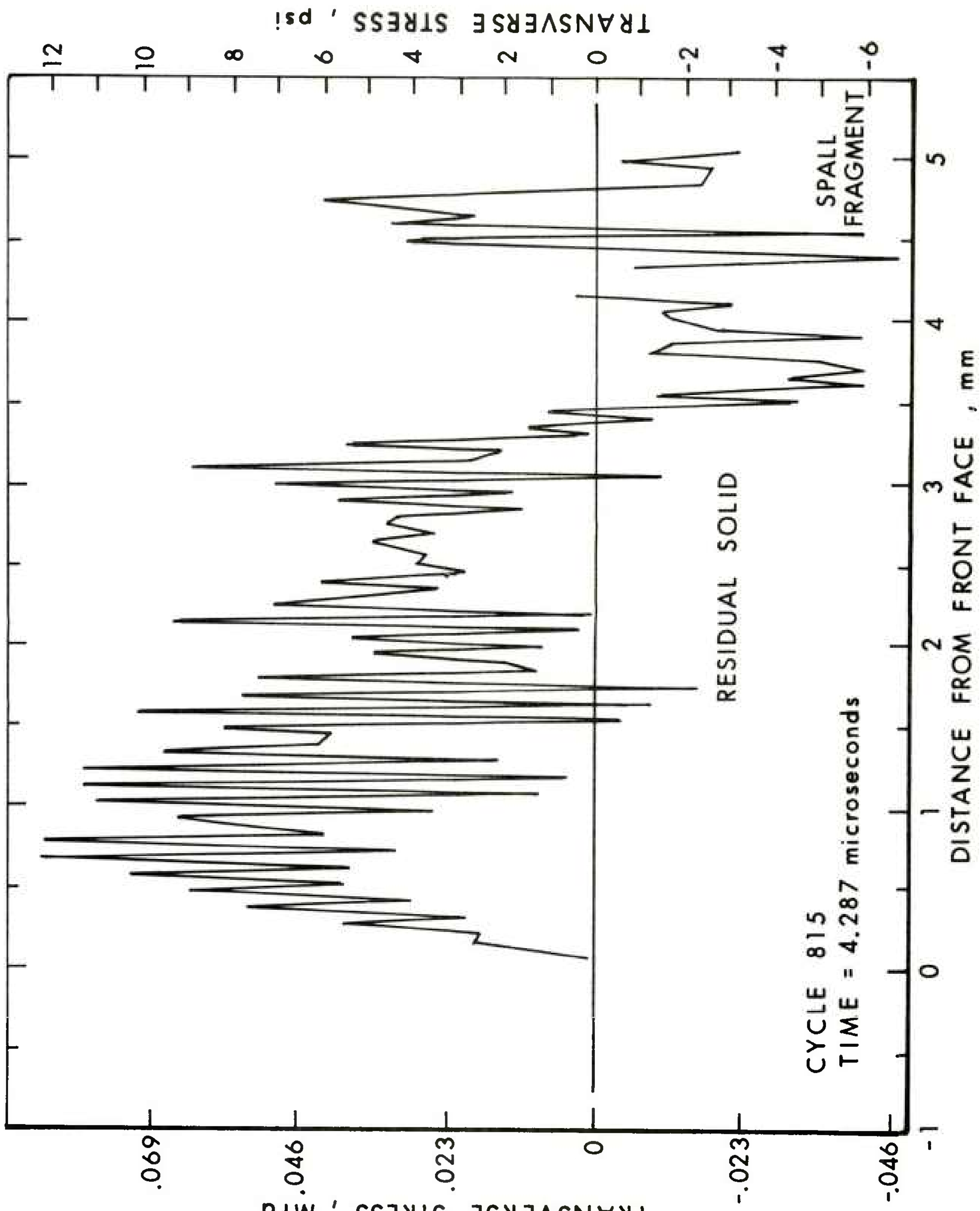

Figure 6. Transverse Stress Distribution

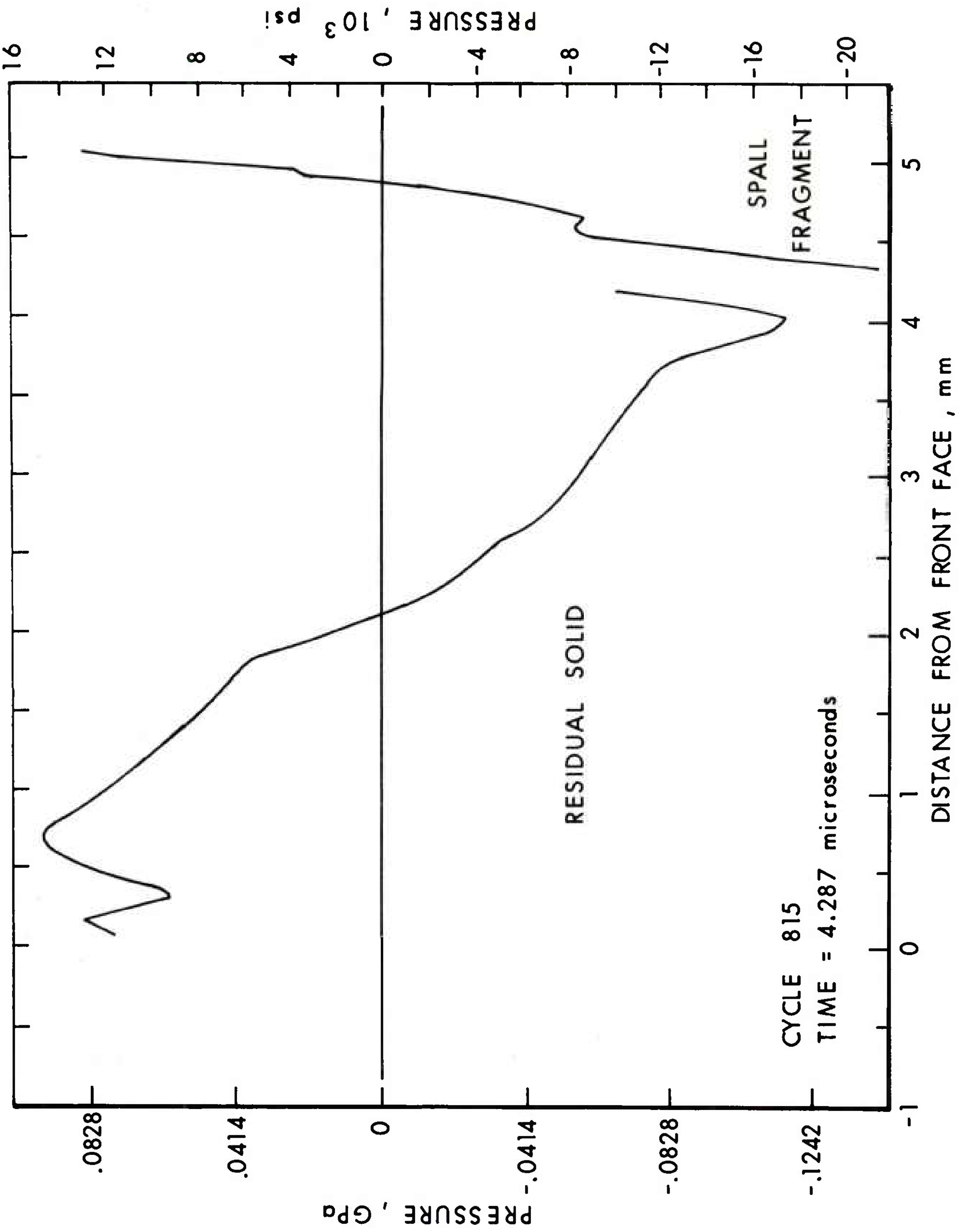

Figure 7. Pressure Distribution

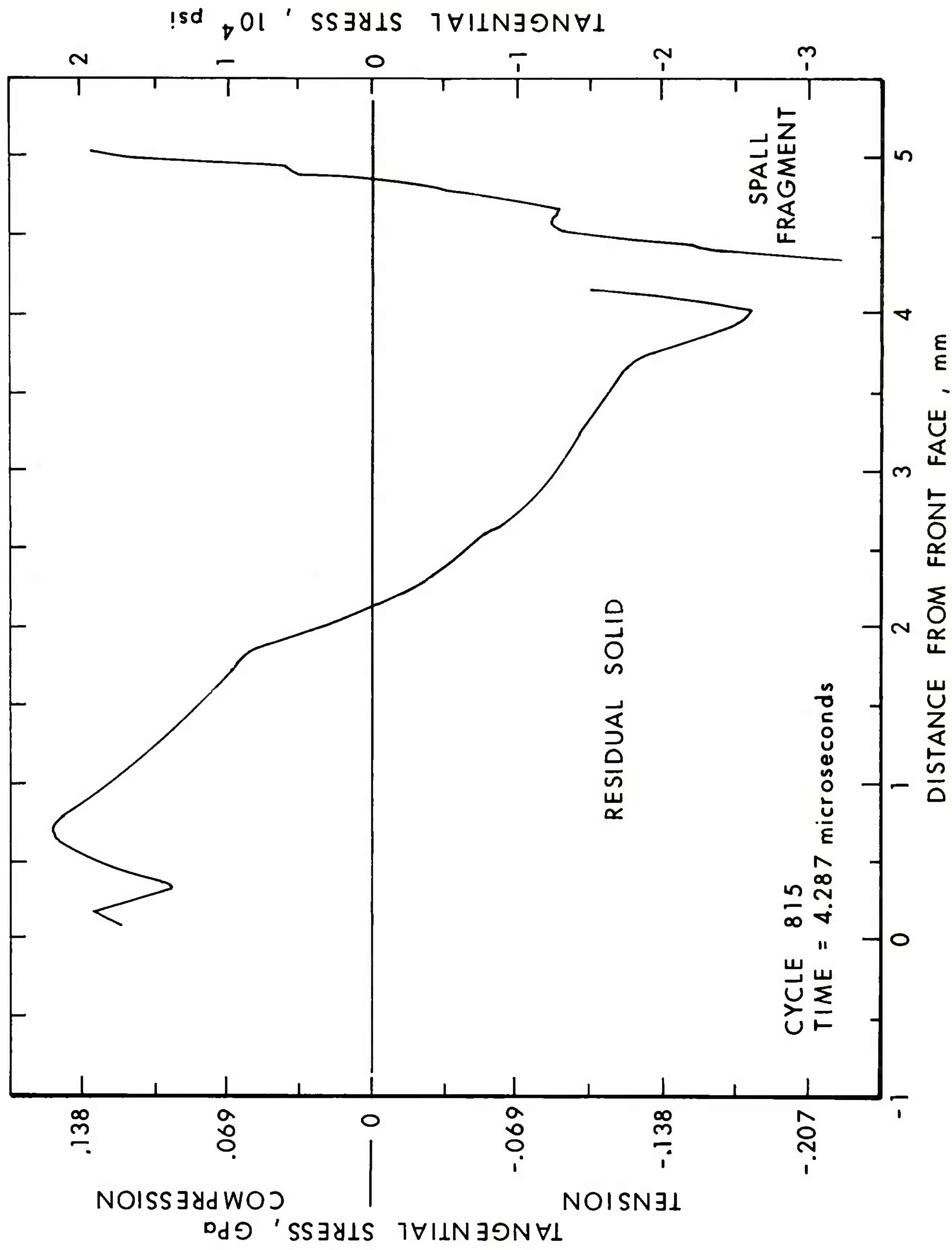

Figure 8. Residual Tangential Stress Distribution

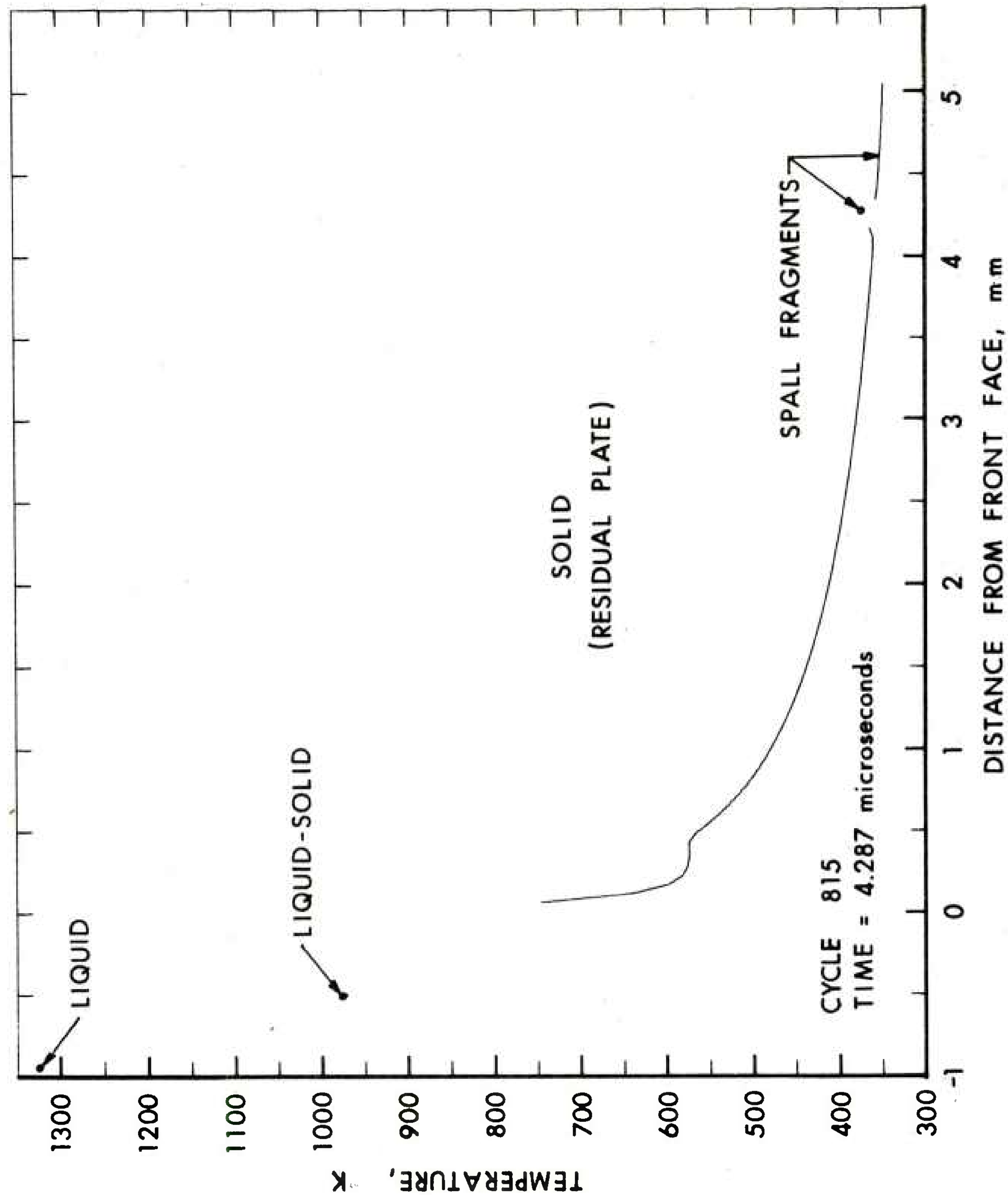

Figure 9. Temperature Distribution

As previously mentioned, damping is introduced into the RIP code calculations after plastic flow and spallation have subsided. This is illustrated in Figure 10, which presents the kinetic energy of the solid material as a function of time. Where there is more than one curve for a period of time, the kinetic energies of the residual material and of one or more spall fragments are displayed individually. The lowest curve gives the kinetic energy of the residual plate. Spallation occurs in the manner illustrated in Figure 5 with separation and coalescence as indicated in Figure 10. This case was initially run without damping to 2,400 nanoseconds (plotted as dashed lines). By examination of this solution it was determined that plastic work and spallation is completed by 1,800 nanoseconds. Therefore it would be satisfactory to introduce damping at 1,800 nanoseconds. This was done in the second run which self-terminated at 4,298 nanoseconds when a criterion for smallness of residual oscillations was satisfied. The corresponding variation of the velocity of the mass center of a portion (to be defined) of the solid material is shown in Figure 11. Since the thickness of residual material was not known until the completion of the calculation, it was not practical to plot the mass center velocity of that material alone. Consequently, Figure 11 includes all the variable mass of solid material which has not spalled off at the particular time. After 2,500 nanoseconds the plot represents the velocity of the residual solid material.

IV. PETROS 3 INPUT AND RESULTS

PETROS 3 code modifications designed to accept the RIP output data are explained in Appendix C. The normal PETROS 3 input is described in Reference 5, pages 160 through 171. To take advantage of symmetry only a quarter of the plate, as shown in Figure 3, is treated. The problem is solved by utilizing a 12 × 16 square mesh with one layer of material and a thickness of 4.093 mm (0.16116 inches) (see Figure 12). An impulsive velocity of 0.83439 m/sec (32.85 in/sec) was distributed uniformly over the surface* of the plate.

In the structural shell response analysis, stresses are calculated ad discrete layers in the through-thickness direction. These calculations can be performed using "room temperature" material properties or thermally degraded properties. For the latter case yield stress[13] and elastic moduli[14]

Along the row of mesh points adjacent to a clamped boundary the PETROS 3 code will modify this initial velocity for compatibility with the finite difference clamped edge boundary condition.

[13] Engineering Data for Aluminum Structures, *The Aluminum Association, New York, N. Y., August 1969.*

[14] *J. Lipkin, J. C. Swearengen, C. H. Karnes, "Mechanical Properties of 6061-T6 Aluminum after Very Rapid Heating," Sandia Laboratories Report SC-RR-72-0020, March 1972.*

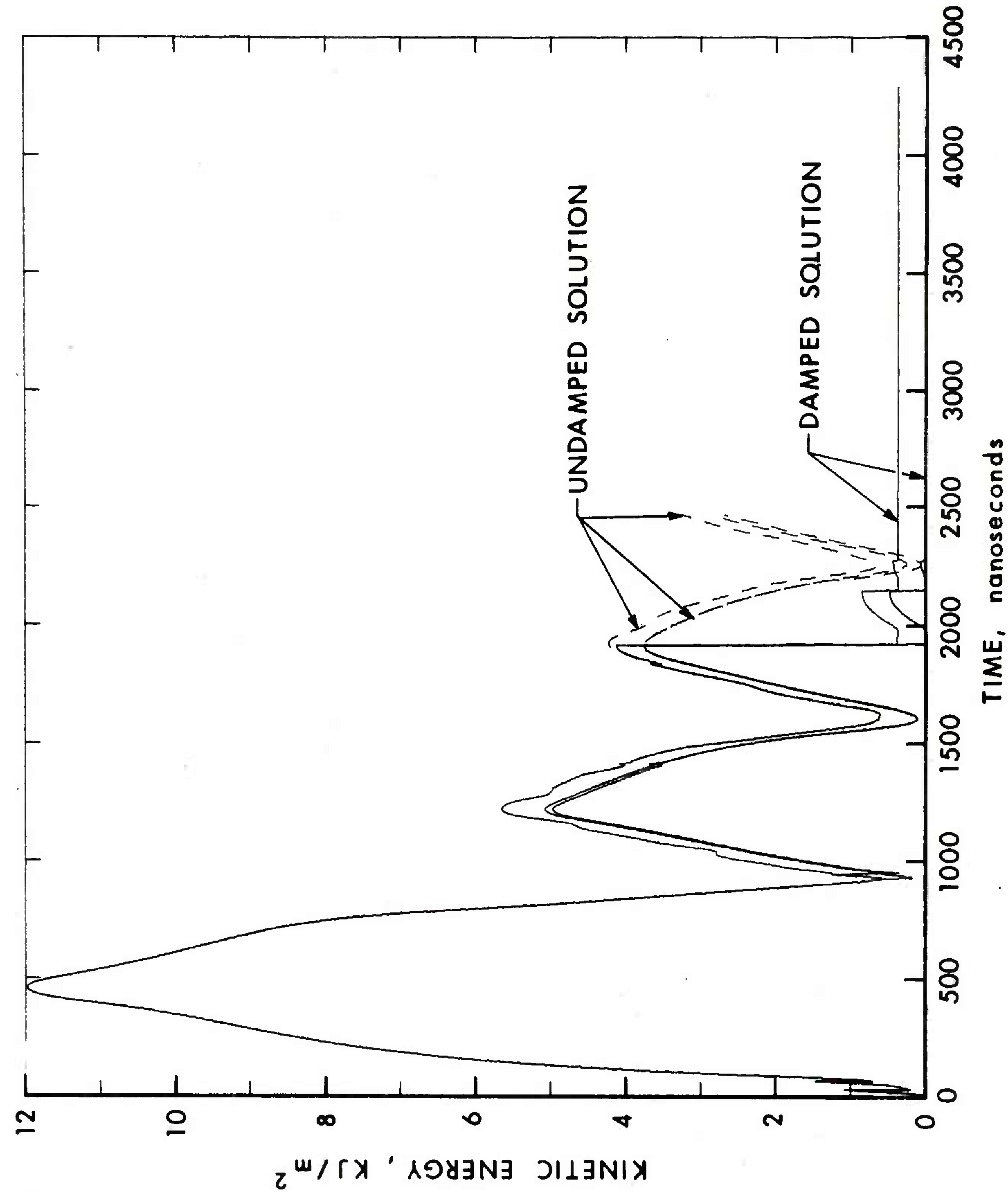

Figure 10. Kinetic Energy of Solid Material

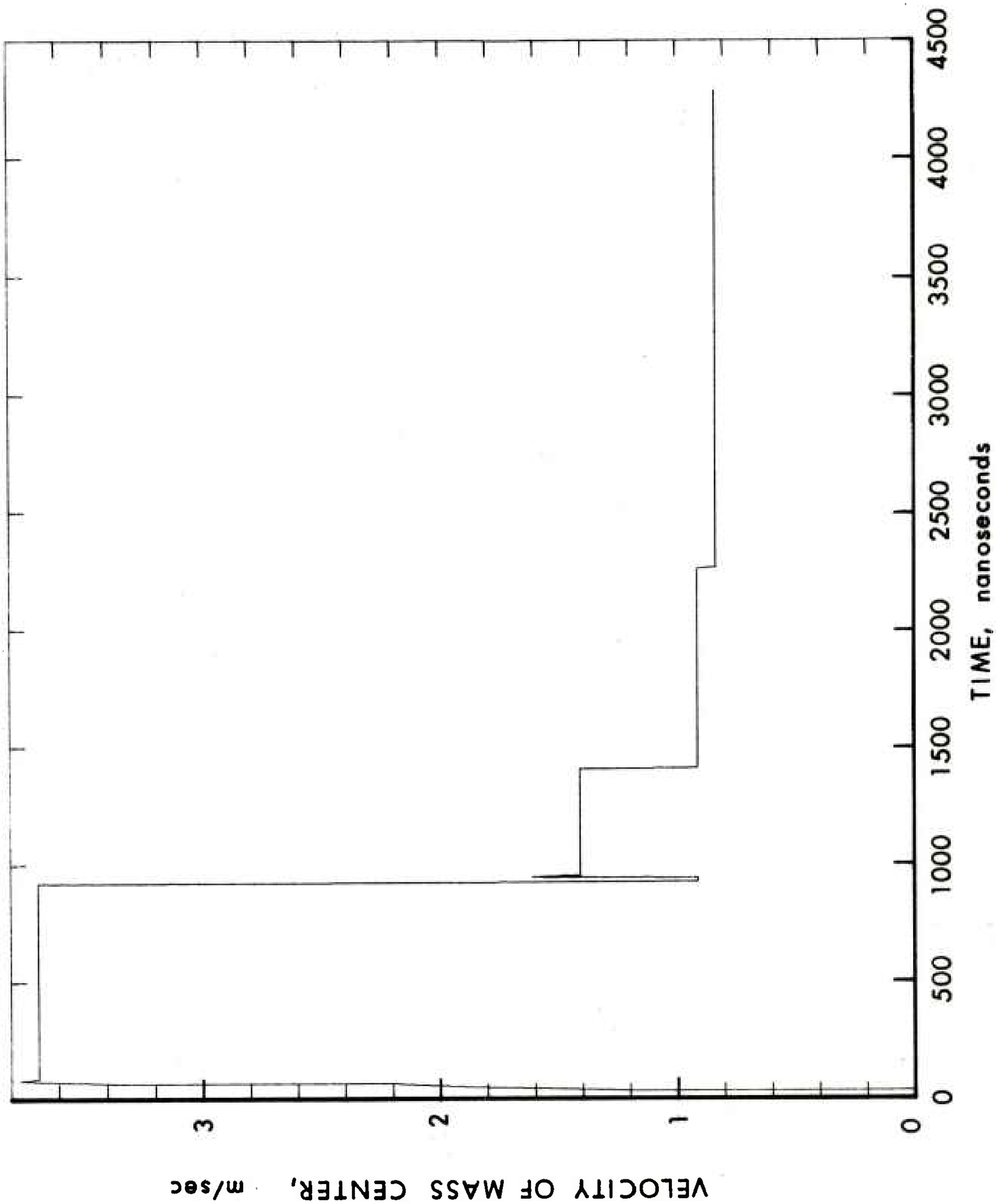

Figure 11. Velocity of Mass Center of Unspalled Solid Material

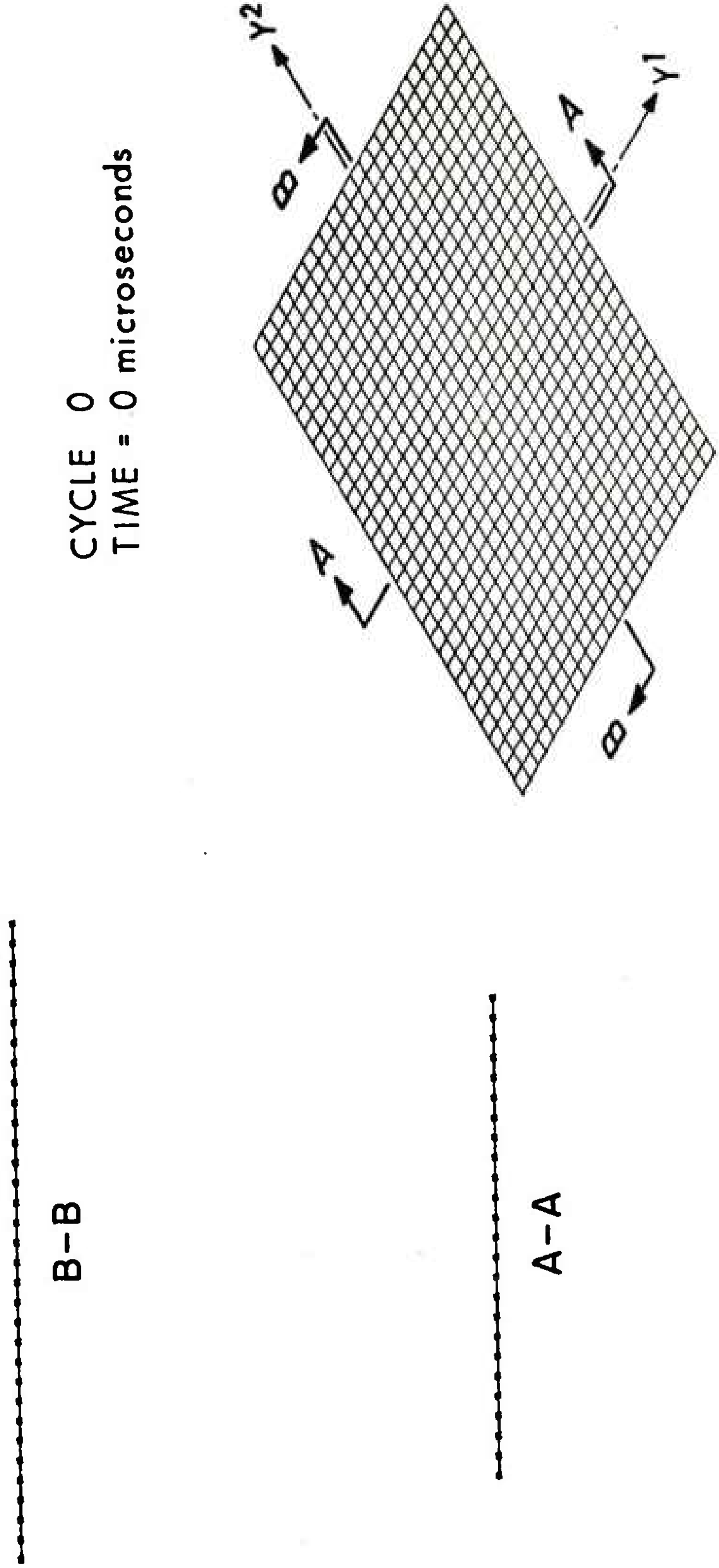

Figure 12. Finite Difference Mesh for Undeformed Plate

as function of temperature, as represented by Figures 13 and 14, were used. Poisson's ratio was calculated as a function of temperature from the data of Figure 14 by the known relationship among the elastic constants of an isotropic material:

$$\nu = \frac{E}{2G} - 1$$

In PETROS 3 a Gaussian quadrature integration as explained in Reference 15, page 41, is used to evaluate the inplane stress and moment resultants at each mesh point. For the results which follow, values of stress at six Gauss points were used for the initial tangential stress through the thickness of the plate. The values of both cold and heated material properties used in these calculations are listed in Table III for each Gauss point through the thickness.

The deflection patterns predicted for cold and heated material properties are compared at two successive times in Figures 15 and 16. On the left of each isometric plot the deformed and undeformed cross-section and profile of the plate can be compared. The deflection of the midpoint of the plate as a function of time is shown in Figure 17. For both solutions, the plate initially moves downward due to the blow-off impulse but the locked-in stresses (from the RIP solution) prevail and the plate eventually assumes a buckled upward configuration. Not surprisingly, the excursions in both directions are greater for the thermally degraded properties solution.

Figure 18 shows elongational strain versus time in the Y^1 and Y^2 directions (see Figure 12) at the center of the plate on the upper and lower surfaces for cold and heated material properties. In comparing these strains, one sees that the largest strain component occurs on the lower surface in Y^1 direction.

Figure 19 shows the energy balance information produced by the PETROS 3 code for the cases under consideration. These results are useful both for detection of possible numerical instabilities and for determining when the solution may be terminated. The information for the cold material properties shows that the response was principally elastic with very little plastic work having taken place during the structural response phase. By contrast, a large amount of plastic work is evident for the solution using thermally degraded material properties. This plastic work can be interpreted as being composed of two parts,

---

[15] *L. Morino, J. W. Leech and E. A. Witmer, "PETROS 2: A New Finite-Difference Method and Program for the Calculation of Large Elastic-Plastic Dynamically-Induced Deformations of General Thin Shells," BRL CR 12 (MIT-ASRL TR 152-1), December 1969. (In two parts: AD 708773 and AD 708774).*

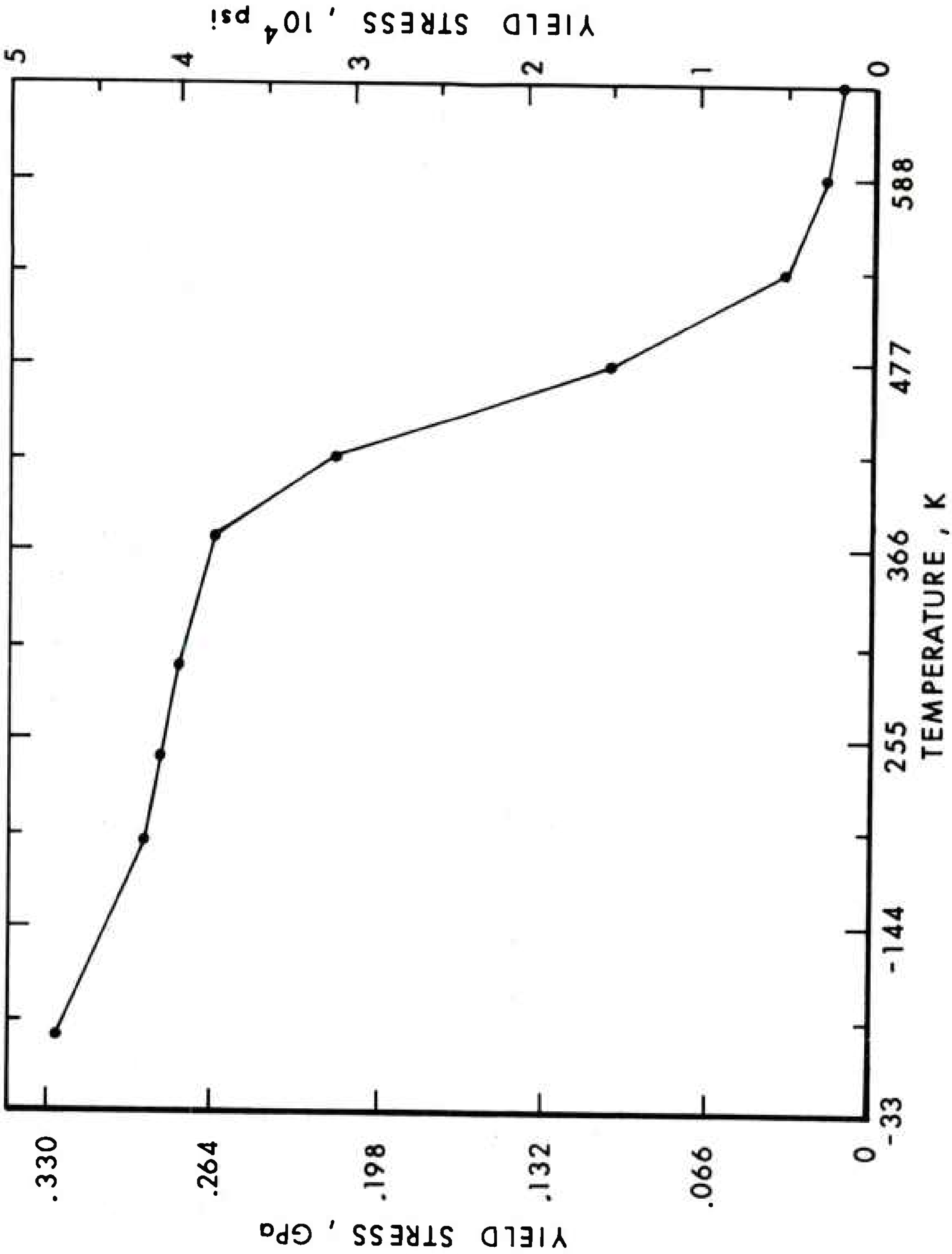

Figure 13. Yield Stress Dependence on Temperature for 6061-T6 Aluminum Alloy

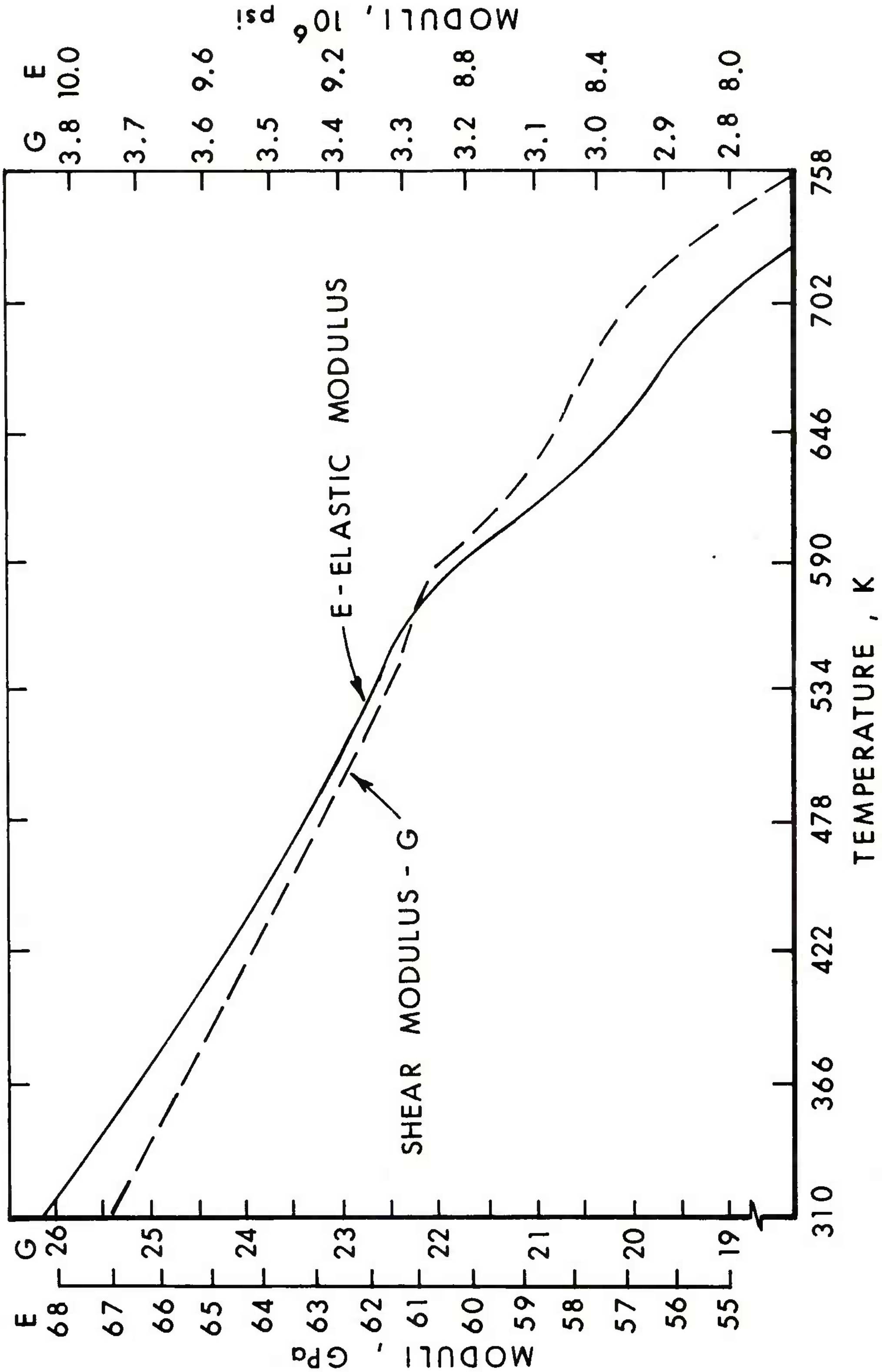

Figure 14. Elastic Moduli of 6061-T6 Aluminum Alloy versus Temperature

Table III

Cold Material Properties (Room Temperature)

G	Distance* mm	Stress GPa	Density Kg/m^3	Elastic Modulus GPa	Poisson's Ratio	Yield Strength GPa
1	.138	-.133	2768.	73.8	.3	.29
2	.693	-.151	2768.	73.8	.3	.29
3	1.558	-.074	2768.	73.8	.3	.29
4	2.535	.050	2768.	73.8	.3	.29
5	3.400	.109	2768.	73.8	.3	.29
6	3.955	.180	2768.	73.8	.3	.29

Heated Material Properties

G	Distance* mm	Temperature K	Stress GPa	Density Kg/m^3	Elastic Modulus GPa	Poisson's Ratio	Yield Strength GPa
1	.138	600.	-.133	2641.	60.1	.367	.017
2	.693	516.	-.151	2660.	63.0	.365	.051
3	1.558	432.	-.074	2676.	65.4	.352	.198
4	2.535	391.	.050	2681.	66.7	.348	.248
5	3.400	371.	.110	2684.	67.4	.347	.264
6	3.955	361.	.179	2684.	67.7	.347	.269

*From front face.

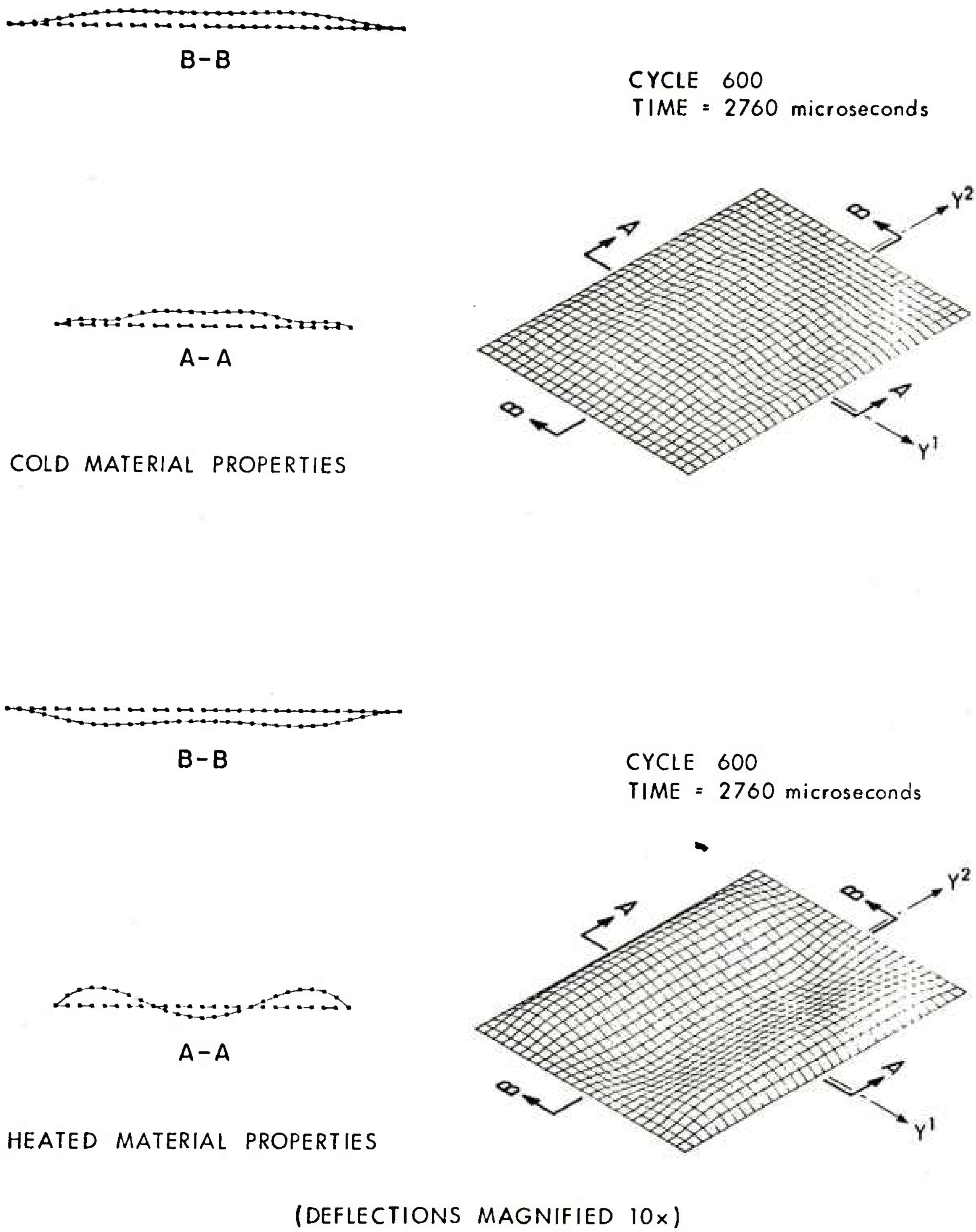

Figure 15. Deformed Reference Surface at Time Step 600

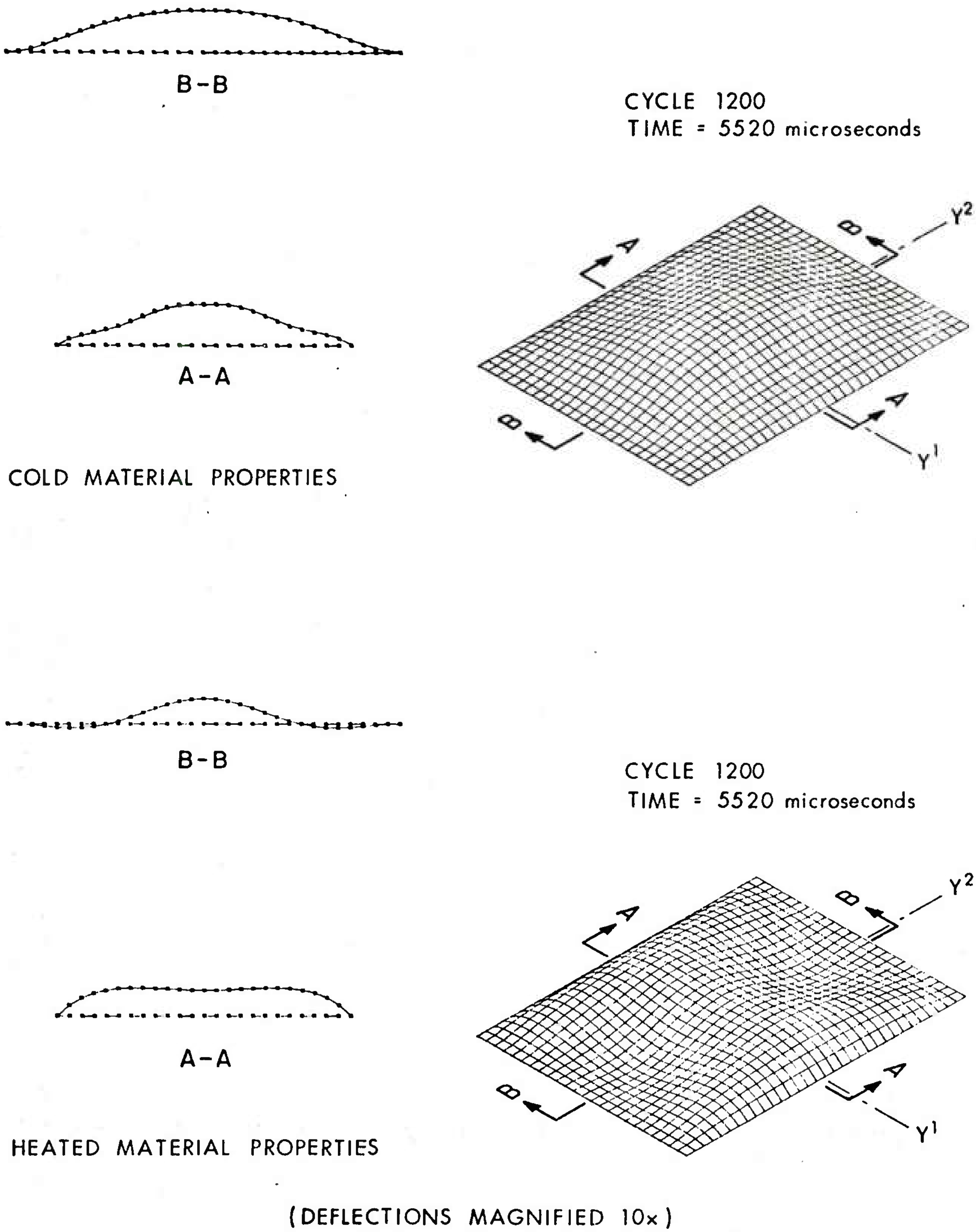

Figure 16. Deformed Reference Surface at Time Step 1200

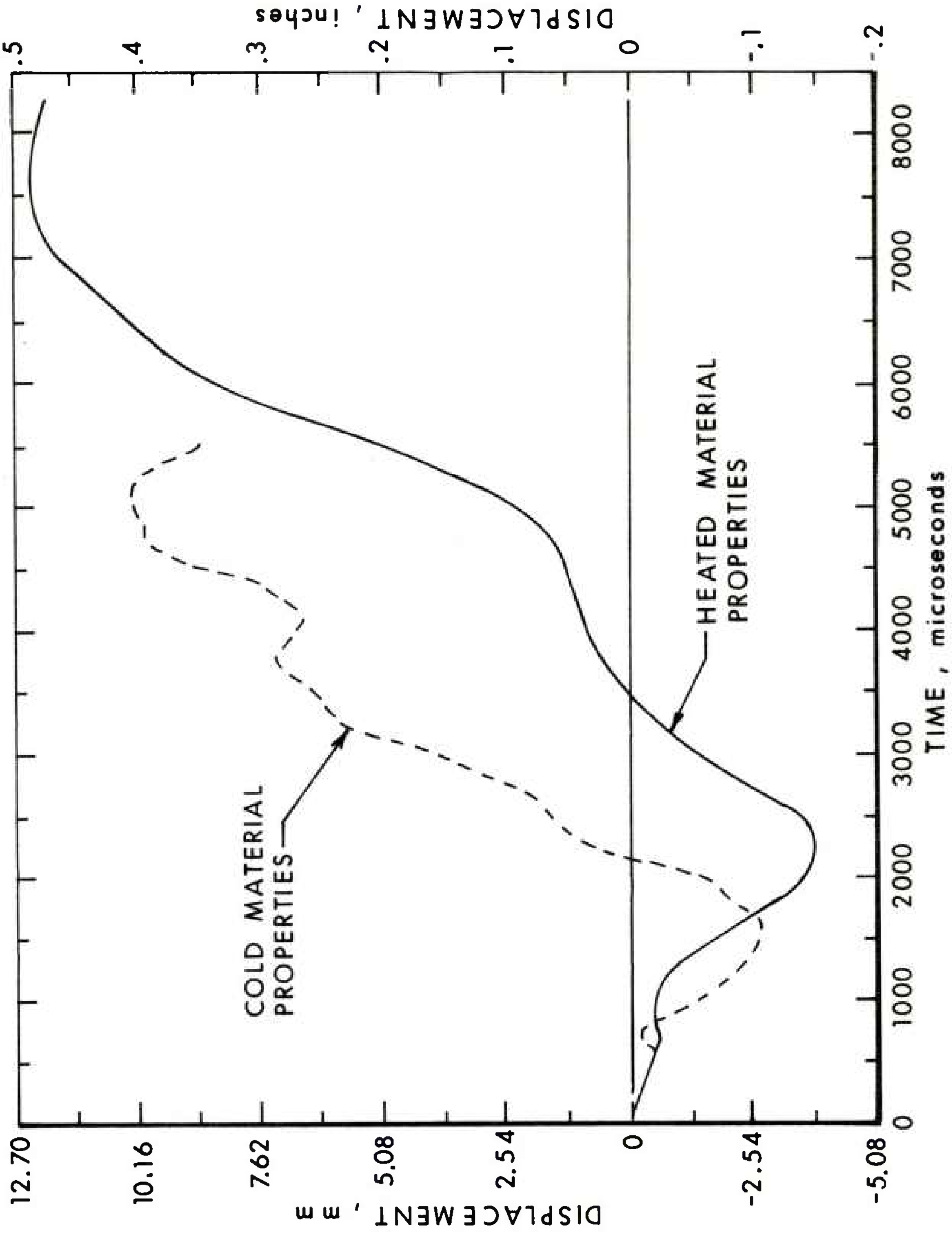

Figure 17. Transverse Displacement of Midpoint of Plate

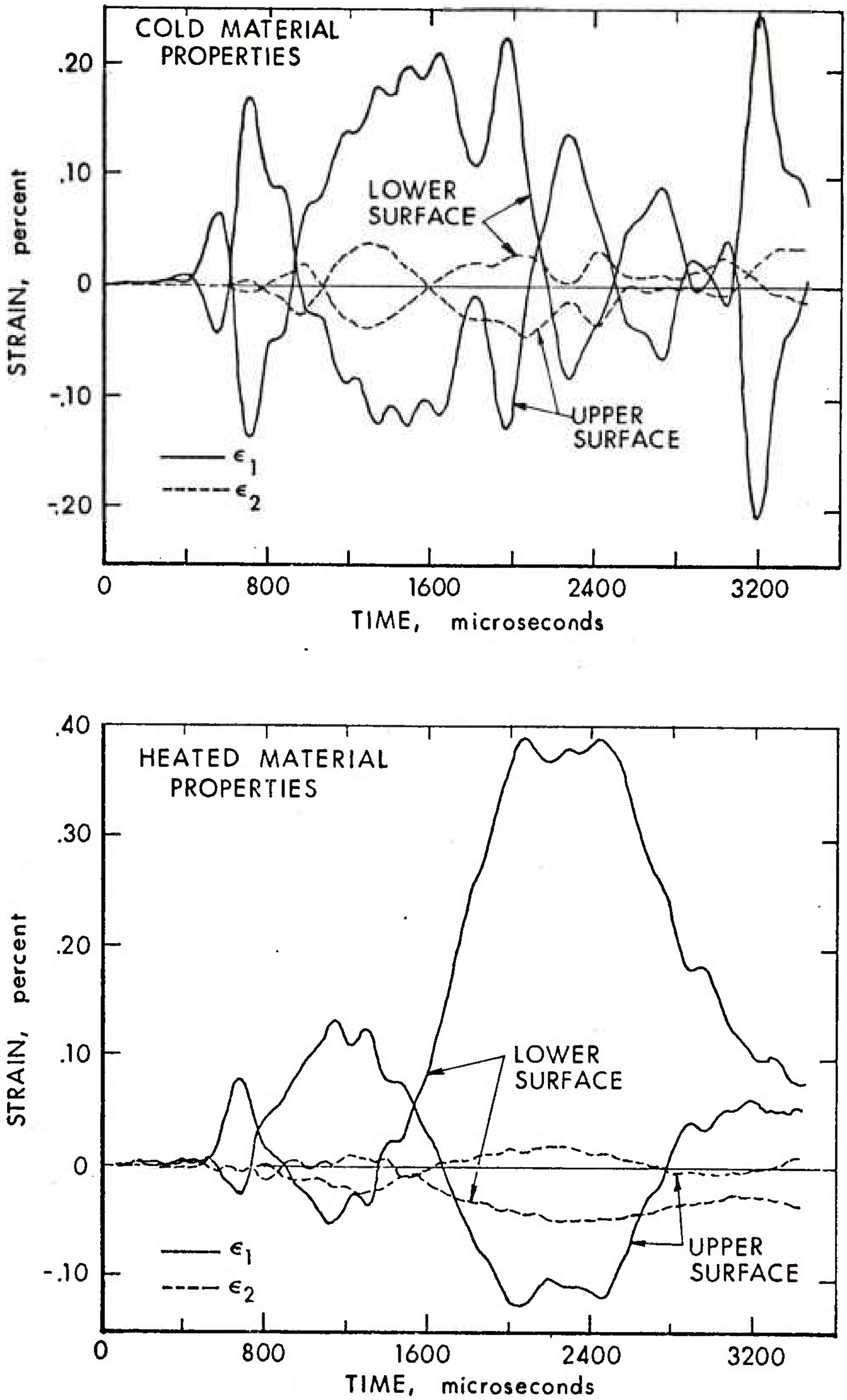

Figure 18. Surface Strain on the Top and Bottom Surface

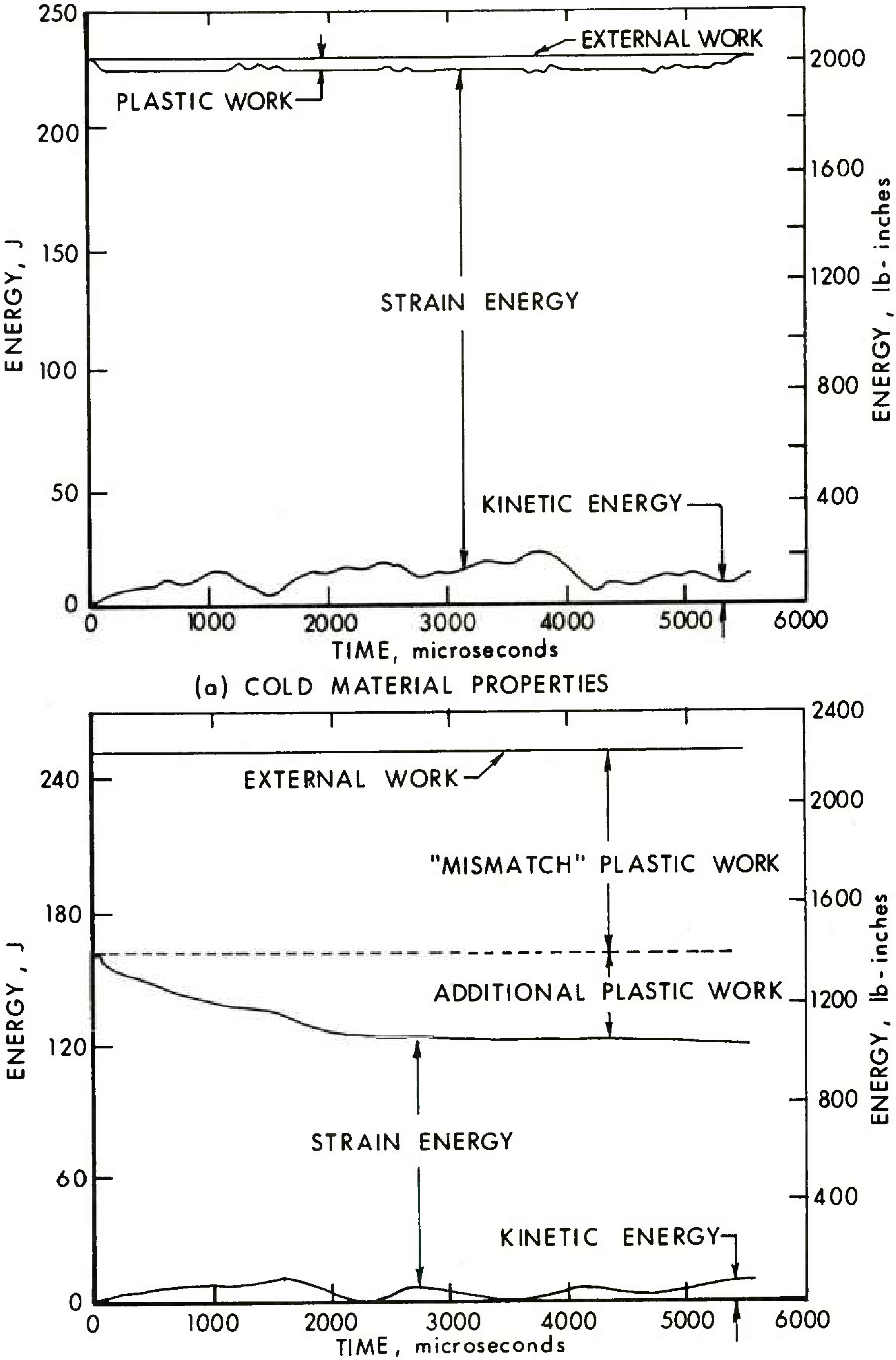

(a) COLD MATERIAL PROPERTIES

(b) HEATED MATERIAL PROPERTIES

interpreted as being composed of two parts, separated by the dashed line in Figure 19(b). Recalling that the initial stresses for the PETROS 3 analysis were obtained from the RIP solution at t_{RF} (which used cold material properties for stress evaluation), it is easy to see that the PETROS 3 analysis would entail large changes in stress during the first time step when thermally degraded properties are used. These essentially discontinuous stress changes entail a significant reduction in strain energy during the first cycle of PETROS 3 calculations and account for the area in Figure 19(b) labeled "mismatch" plastic work. This non-physical discontinuous change could have been avoided if the RIP code had provision for using thermally degraded material strength properties. The additional plastic work associated with the structural response phase, using thermally weakened material characteristics is essentially complete by the termination of the solution. The increase in external work is due to the change in Poisson's ratio from cold to heated material properties.

It should be noted that the PETROS 3 calculations were performed using the temperature distribution of Figure 9 as though the temperature were invariant for the duration of the structural response prediction. A discussion of this point is presented in Appendix D.

V. CONCLUSION

The present work illustrates a procedure for predicting the structural response of target structures after intense, rapid heating due to x-ray radiation deposition. It is evident from comparing the solutions of the undegraded material properties and the degraded material properties that the results are significantly different. This indicates that precise modeling of structural response in rapid heating situations requires an accurate definition of degraded material properties under such conditions.

The methodology described is not limited to cases solved here. Other initial geometries with multilayer hard bonded material could be analyzed in a similar manner.

ACKNOWLEDGMENT

The author acknowledges Dr. Norris J. Huffington, Jr. and Dr. Joseph M. Santiago for their helpful advice and criticism, Mr. Fred Gregory for his assistance in obtaining RIP input data, Mr. Joseph Lacetera and Mrs. Janet Lacetera for their helpful discussions related to the RIP program, and Mr. Ennis F. Quigley for the results presented in Appendix D.

REFERENCES

1. R. H. Fisher, G. A. Lane, and R. A. Cecil, "RIP, A One-Dimensional Material Response Code - User's Guide," Systems, Science and Software, Report 3SR-751-I, September 1972.

2. R. H. Fisher, G. A. Lane, and R. A. Cecil, "RIP, A One-Dimensional Material Response Code - Code Reference Manual," Systems, Science and Software, Report 3SR-751-II, September 1972.

3. R. A. Kruger, "The Material Response Program, RIP," Systems, Science and Software, Report 3SR-120, December 1969.

4. RIP, A One-Dimensional Material Response Code. Systems, Science and Software, Contract No. SSS-R-72-1324.

5. S. Atluri, E. A. Witmer, J. W. Leech, and L. Marino, "PETROS 3: A Finite Difference Method and Program for the Calculation of Large Elastic-Plastic Dynamically Induced Deformations of Multilayer Variable - Thickness Shells," U.S. Army Ballistic Research Laboratories, Contract Report No. 60, November 1971 (AD# 890200L).

6. J. M. Santiago, H. L. Wisniewski, N. J. Huffington, Jr., "A User's Manual for the REPSIL Code." U.S. Army Ballistic Research Laboratories, Report no. 1744, October 1974. (AD #A003176)

7. B. J. Kohn, "Compilation of Hugoniot Equations of State," Air Force Weapons Laboratory, April 1969 (page 19).

8. Sensitivity of Material Response Calculations to the Equation of State Model, Systems, Science and Software, Contract Report No. 130 (SSS-R-73-1910), December 1973 (page 24).

9. E. B. Royce, "Gray, A Three-Phase Equation of State for Metals," Lawrence Livermore Laboratory, Report UCRL-51121, September 1971 (page 38).

10. R. B. Oswald, Jr., F. B. McLean, D. R. Schallhorn, and T. R. Oldham, "The Dynamic Response of Aluminum to Pulsed Energy Deposition in the Melt-Dominated Regime," U.S. Harry Diamond Laboratories, HDL-TR-1624, July 1973 (page 11).

11. R. H. Fisher and J. W. Wiehe, "A User's Guide to the FSCATT Code," Systems, Science and Software, Report 3SR-318, November 1970.

12. R. H. Fisher and R. A. Kruger, "A Numerical Treatment of Scattering and Fluorescence in Plane Geometry," Systems, Science and Software, Report 3SR-119, September 1969.

13. Engineering Data for Aluminum Structures, The Aluminum Association, New York, N. Y., August 1969.

14. J. Lipkin, J. C. Swearengen, C. H. Karnes, "Mechanical Properties of 6061-T6 Aluminum after Very Rapid Heating," Sandia Laboratories Report SC-RR-72-0020, March 1972.

15. L. Morino, J. W. Leech and E. A. Witmer, "PETROS 2: A New Finite-Difference Method and Program for the Calculation of Large Elastic-Plastic Dynamically-Induced Deformations of General Thin Shells," BRL CR 12 (MIT-ASRL TR 152-1), December 1969. (In two parts: AD 708773 and AD 708774).

16. M. W. Coleman and J. V. Lanaham, "BRLESC FORTRAN Plotting Subroutines," Aberdeen Research and Development Center, Technical Report No. 6, June 1970.

17. J. D. Gask, "Chrysler Improved Numerical Differencing Analyser for Third Generation Computers," Chrysler Corporation Space Division, TN-AP-67-287, October 20, 1967.

APPENDIX A

CODING CHANGES TO RIP

Two types of changes to the RIP program listed in Reference 2 were needed in order to couple RIP and PETROS 3. The first change was designed to extract data to assist in interpreting the RIP output needed as PETROS 3 input. The second was to extract temperature from the Gray equations of state, and change the momentum editing flags to agree with the Gray equation of state editing flags, which determine within which region the calculation point lies.

A list is provided with a description of variables used in subroutine DAMP, PDATA, and PETINP. They are constructed to speed the process of determining the solution and provide additional output not contained in the normal RIP output format. Following this list is a brief explanation and FORTRAN listing of the subroutines.

CHANGES TO THE RIP PROGRAM TO OBTAIN PLOTTING DATA FOR THE BRL RIP PLOTTING PROGRAM

```
1. FOLLOWING CARD RIP1270 ADD THE FOLLOWING
      IF(NRESRT .EQ. 0)CALL PDATA(1)

2. FOLLOWING CARD RIP1310 ADD THE FOLLOWING
      CALL PDATA(1)

3. FOLLOWING CARD RIP1370 ADD THE FOLLOWING STATEMENTS
      CALL EDIT
      CALL TDELT

4. FOLLOWING CARD RIP2190 ADD THE FOLLOWING STATEMENTS
  180 CALL PDATA(2)
      CALL EDIT
      CALL TDELT
      CALL PDATA(5)

   REMOVE CARD RIP2200 WHICH STATES
  180 CALL EDIT
5. FOLLOWING CARD EDI 950 ADD THE FOLLOWING
      CALL PDATA(4)

6. FOLLOWING CARD EDI1410 ADD THE FOLLOWING
      CALL PETINP
      IF(NSEDIT .EQ. 0)CALL PDATA(3)
      CALL EXIT

   REMOVE CARD EDI1420 WHICH STATES
      IF(NSEDIT .EQ. 0)CALL EXIT
```

CHANGES TO THE MOMENTUM EDITING FLAGS IN SUBROUTINE ENCALE

```
1. CODING WHICH FOLLOWS LINE
      TEMP(1)=TIME-DTNP1                                          ENC1440

   ADD LINE
      GOTO (142,142,146,146),IEOS

   AND CHANGE THE STATEMENT WHICH STATES
      IF(E(J) .GE. ESTCON(10,N))MZONE(M,1)=J                       ENC1460

   TO THE FOLLOWING
  142 IF(E(J) .GE. ESTCON(10,N))MZONE(M,1)=J

2. CODING WHICH FOLLOWS LINE
      IF(E(J) .GE. ESTCON(13,N))MZONE(M,4)=J                       ENC1490

   ADD LINES
      GOTO 150
C                     FOR GRAY E.O.S. ONLY
  146 IF(IVFLAG(J) .EQ. 35)MZONE(M,1)=J
      IF(IVFLAG(J) .EQ. 33)MZONE(M,2)=J
      IF(IVFLAG(J) .EQ. 32)MZONE(M,3)=J
      IF(IVFLAG(J) .EQ. 31)MZONE(M,4)=J
```

CHANGES FOR EXTRACTING TEMPERATURE FROM THE GRAY EQUATION OF STATE SUBROUTINE EOS3

```
1. CODING WHICH FOLLOWS LINE
   .        U(1000),X(1000),BLANK(39)                                ESC 210

   ADD LINE
      COMMON /EOSMAT/GTEMP(1000)

2. CODING WHICH FOLLOWS LINE
      P(J)=TEM(4)*TEMP(5)-TEMP(7)+TEMP(9)*TEMP(10)                  ESC2190
   ADD LINE
      TEMP(5)=TEMP(8)

3. CODING WHICH FOLLOWS LINE
      P(J)=1.E+12*P(J)                                              ESC2240
   ADD LINE
      GTEMP(J)=TEMP(5)
```

CHANGES FOR PRINTING TEMPERATURE IN SUBROUTINE MECIT

```
1. CODING WHICH FOLLOWS LINE
   .        U(1000),X(1000),BLANK(39)                                MDT 210
   ADD LINE
      COMMON /EQSMAT/GTEMP(1000)

2. CHANGE THE STATEMENT WHICH STATES
      PRINT 130,J,SMASS,X(J),U(J),RHO(J),Q(J),PT,P(J),E(J),C(J)     MDT 390
   .        IVFLAG(J),IBFLAG(J),J                                   MDT 400
   TO THE FOLLOWING
      PRINT 130,J,SMASS,X(J),U(J),RHO(J),SD(J),S(J),P(J),E(J),GTEMP(J),
   .        IVFLAG(J),IBFLAG(J),J

3. CHANGE FORMAT 100 TO THE FOLLOWING
  100 FORMAT(1H1,4X,12A6,5X,11HCYCLE NO. =I5,2X,6HTIME =1PE13.5//4X,
     .1HJ,4X,5HSMASS,8X,1HX,10X,1HU,10X,3HRHO,7X,2HSD,9X,1HS,11X,
     .1HP,10X,1HE,10X,1HT,8X,2HIV,2X,2HIB,4X,1HJ/)

4. CHANGE FORMAT 140 TO THE FOLLOWING
  140 FORMAT(1H1,3X,1HJ,4X,5HSMASS,8X,1HX,10X,1HU,10X,3HRHO,7X,2HSD,9X,
     .1HS,11X,1HP,10X,1HE,10X,1HT,8X,2HIV,2X,2HIB,4X,1HJ/)
```

Subroutine PDATA, DAMP, and PETINP Local Variables

Name	Definition
CMTOIN	Constant to convert centimeters to inches.
CIN1	Kinetic energy of the vapor-liquid region.
CIN2	Kinetic energy of the liquid region.
CIN3	Kinetic energy of the liquid solid region.
CINET	Total kinetic energy of all regions.
CINS(20)	Kinetic energy of each solid piece KF, after spallation.
DCPSI	Constant to convert dynes/cm^2 to psi.
DFACT	Minimum average transverse stress used to control the termination of the problem during damping (Input card 4).
DSTOP(20)	Control if DSTOP(I) = 1 solid piece has been damped, DSTOP(I) = 0 continue damping.
EERGY	Internal energy plus kinetic energy for all regions.
GCTOLB	Constant to convert g/cm^2 to lb-sec^2/$in.^4$.
GTEMP(J) J = 1, 1000	Temperature of Zone J (K).
I	Counter.
IFIRST	Control variable governing mode of operations.
IFLAG	Control variable (see description of variables in Appendix B).
J	Counter.
JK	Counter for indexing array JSS(JK).
JS	Initial count used in DO statement in subroutine DAMP.
JSN	Final count used in DO statement in subroutine DAMP.
JSS(40)	Zone numbers corresponding to the first and last zone of each solid piece. JSS(JK) = First zone of the KF solid piece. JSS(JK + 1) = Final zone of the KF solid piece.

KEY	Control variable governing mode of operations.
KF	Number of solid pieces after spallation.
KINET1(20)	Kinetic energy at time t - Δt for the KF solid piece.
KINET2(20)	Kinetic energy at time t for each solid piece KF.
LINK	Control number used in subroutine PDATA.
LMAXP	Number of times at which profile plots are drawn (Input card 2 needed for plotting).
LTP	Control number.
NCOM(20)	Control number to check if two solid pieces have recombined after they had previously spalled.
NP	Number of time steps at which profile plots are drawn (Input card 1 needed for plotting).
NPOLT	Plotting tape unit number.
NT	Counter.
NTIME(50)	Time steps at which profile plots are obtained (Input card 1).
SMASS	Sum of the masses in the solid region.
SUMKIN(20)	Sum of kinetic energies of the solid region.
TANGS	Tangential stress.
TDAMP	Time at which damping starts (Input card 4).
TEMF	Temperature in (°F).
THICK	Thickness.
THICK1	Spatial coordinate of the first zone of the KF solid piece.
TPLOT(50)	Times at which profile plots are obtained (Input card 3).
TRANS	Average transverse stress.
VCEN(20)	Array containing the velocity of the mass center of each solid piece KF.
VCENT	Same as VCEN(20).
VCENTR	Velocity of the mass center of the first KF.

Explanation of Subroutines

PDATA — Along with the RIP input data, Table I, the following input data is needed to obtain data on tape. Also this subroutine calculates and stores the data on tape required by the BRL-RIP plotting program. Appendix B describes and lists the program.

Input Data

Card	Variables	Format
1	NP, (MTIME(I), I = 1, NP)	16I5
2	LMAXP	16I5
3	(TPLOT(I), I = 1, LMAXP)	16I5
4	TDAMP, DFACT	2E12.6

Description of Input

Card 1	NP	Number of time steps for which timewise plots of transverse stress, tangential stress, pressure and temperature are plotted.
	NTIME(I)	Time steps that transverse stress, tangential stress, pressure and temperature are plotted.
Card 2	LMAXP	Number of times for which timewise plots of transverse stress, tangential stress, pressure and temperature are plotted.
Card 3	TPLOT(I)	Times that transverse stress, tangential stress, pressure and temperature are plotted.
Card 4	TDAMP	Time at which damping starts. See Reference 9, page 59, for a more detailed explanation of TDAMP.
	DFACT	Minimum average transverse stress value used to control the termination of the problem during damping.

DAMP — As already mentioned in the Calculational Procedure, this subroutine is patterned on subroutine DAMP, Reference 6, page 46, except that no energy is dissipated by viscous damping, all the kinetic energy is reduced by the kinetic energy annihilation procedure. This procedure involves freezing the zone velocity of the material to the velocity of the mass center whenever the kinetic energy of the material reaches a maximum. Therefore, the vibratory kinetic energy of the material is made to vanish and the total kinetic energy reduced to the translational kinetic energy of the mass center. Then the material is released with less energy. The above is repeated until the average transverse stress is less than DFACT. If spallation in the solid region takes place, each solid portion is damped separately.

PETINP At the termination of the run, this subroutine calculates and outputs the physical properties of the remaining solid portions of material (See Table A-1) which are needed by PETROS 3 as initial conditions.

Table A-1. RIP Output Summarizing the PETROS 3 Input

PETROS INPUT

SPALL FRAGMENT = 1
VELOCITY OF MASS CENTER = .328588E 02 KINETIC E = .386142E 04

J	X (INCHES)	TRANSVERSE STRESS (PSI)	TANGENTIAL STRESS (PSI)	BULK MODULUS (PSI)	DENSITY	TEMPERATURE
5	.286972E-02	.356563E-01	-.171926E 05	.991661E 07	.243965E-03	.884188E 03
6	.490975E-02	.177426E 01	-.181215E 05	.101072E 08	.246288E-03	.691115E 03
7	.693053E-02	.265638E 01	-.192885E 05	.101796E 08	.247166E-03	.617691E 03
8	.894413E-02	.251745E 01	-.172411E 05	.102030E 08	.247454E-03	.589684E 03
9	.109554E-01	.553275E 01	-.152215E 05	.102100E 08	.247541E-03	.578963E 03
10	.129659E-01	.284710E 01	-.135297E 05	.102110E 08	.247557E-03	.574988E 03
11	.149764E-01	.767660E 01	-.143511E 05	.102132E 08	.247582E-03	.574124E 03
12	.169866E-01	.401311E 01	-.165541E 05	.102165E 08	.247618E-03	.574453E 03
13	.189965E-01	.896145E 01	-.183026E 05	.102304E 08	.247784E-03	.562684E 03
14	.210051E-01	.549617E 01	-.196145E 05	.102540E 08	.248068E-03	.539993E 03
15	.230114E-01	.103269E 02	-.206820E 05	.102753E 08	.248324E-03	.519218E 03
16	.250156E-01	.537024E 01	-.215400E 05	.102945E 08	.248556E-03	.500237E 03
17	.270179E-01	.122974E 02	-.219507E 05	.103114E 08	.248760E-03	.482872E 03
18	.290186E-01	.439690E 01	-.218316E 05	.103261E 08	.248938E-03	.467040E 03
19	.310179E-01	.122163E 02	-.212850E 05	.103387E 08	.249092E-03	.452535E 03
20	.330160E-01	.591080E 01	-.204535E 05	.103498E 08	.249227E-03	.439272E 03
21	.350129E-01	.813348E 01	-.196071E 05	.103597E 08	.249349E-03	.427178E 03
22	.370089E-01	.921013E 01	-.187914E 05	.103687E 08	.249458E-03	.416177E 03
23	.390040E-01	.355247E 01	-.180423E 05	.103770E 08	.249560E-03	.405956E 03
24	.409983E-01	.109734E 02	-.173155E 05	.103849E 08	.249658E-03	.396133E 03
25	.429918E-01	.119581E 01	-.166274E 05	.103925E 08	.249750E-03	.386841E 03
26	.449846E-01	.114176E 02	-.159608E 05	.103995E 08	.249836E-03	.378081E 03
27	.469766E-01	.534390E 00	-.153337E 05	.104062E 08	.249918E-03	.369828E 03
28	.489681E-01	.111907E 02	-.146965E 05	.104124E 08	.249994E-03	.362009E 03
29	.509589E-01	.200079E 01	-.141081E 05	.104183E 08	.250066E-03	.354613E 03
30	.529492E-01	.951144E 01	-.134817E 05	.104237E 08	.250133E-03	.347685E 03
31	.549389E-01	.605653E 01	-.129195E 05	.104289E 08	.250196E-03	.341123E 03
32	.569281E-01	.586300E 01	-.123232E 05	.104337E 08	.250255E-03	.334895E 03
33	.589169E-01	.823557E 01	-.117596E 05	.104383E 08	.250312E-03	.328979E 03
34	.609052E-01	-.677231E 00	-.112336E 05	.104426E 08	.250365E-03	.323301E 03
35	.628930E-01	.100444E 02	-.107072E 05	.104468E 08	.250417E-03	.317827E 03
36	.648805E-01	-.130240E 01	-.101850E 05	.104508E 08	.250466E-03	.312561E 03
37	.668676E-01	.787688E 01	-.968894E 04	.104547E 08	.250513E-03	.307532E 03
38	.680543E-01	-.234712E 01	-.928576E 04	.104584E 08	.250559E-03	.302766E 03
39	.708406E-01	.754370E 01	-.886126E 04	.104620E 08	.250603E-03	.298153E 03
40	.728266E-01	.110207E 01	-.821242E 04	.104651E 08	.250641E-03	.293688E 03
41	.748123E-01	.210568E 01	-.685124E 04	.104670E 08	.250667E-03	.289297E 03
42	.767978E-01	.492710E 01	-.515550E 04	.104682E 08	.250684E-03	.285125E 03
43	.787831E-01	.111253E 01	-.351117E 04	.104693E 08	.250700E-03	.281117E 03
44	.807683E-01	.543446E 01	-.225231E 04	.104708E 08	.250720E-03	.277324E 03
45	.827534E-01	.304993E 00	-.888539E 03	.104720E 08	.250737E-03	.273696E 03
46	.847383E-01	.920917E 01	.643682E 03	.104728E 08	.250750E-03	.270155E 03
47	.867231E-01	.252626E-01	.211211E 04	.104736E 08	.250762E-03	.266759E 03
48	.887079E-01	.715619E 01	.309914E 04	.104751E 08	.250782E-03	.263457E 03
49	.906924E-01	.488688E 01	.385713E 04	.104769E 08	.250805E-03	.260229E 03
50	.926768E-01	.343853E 01	.453886E 04	.104787E 08	.250828E-03	.257092E 03
51	.946610E-01	.611903E 01	.527606E 04	.104803E 08	.250848E-03	.254064E 03
52	.966451E-01	.295806E 01	.603215E 04	.104819E 08	.250868E-03	.251070E 03
53	.986290E-01	.401802E 01	.654949E 04	.104837E 08	.250892E-03	.248153E 03
54	.100613E 00	.373512E 01	.707228E 04	.104855E 08	.250914E-03	.245300E 03

Table A-1. RIP Output Summarizing the PETROS 3 Input (Cont'd)

55	.102596E 00	.441249E 01	.783912E 04	.104868E 08	.250931E-03	.242594E 03
56	.104580E 00	.493887E 01	.887775E 04	.104876E 08	.250943E-03	.239924E 03
57	.106563E 00	.358567E 01	.979207E 04	.104886E 08	.250956E-03	.237338E 03
58	.108546E 00	.469519E 01	.103625E 05	.104899E 08	.250973E-03	.234880E 03
59	.110529E 00	.434038E 01	.109417E 05	.104912E 08	.250990E-03	.232477E 03
60	.112512E 00	.162109E 01	.114404E 05	.104926E 08	.251007E-03	.230163E 03
61	.114495E 00	.570308E 01	.119429E 05	.104938E 08	.251023E-03	.227916E 03
62	.116478E 00	.184327E 01	.123785E 05	.104952E 08	.251040E-03	.225715E 03
63	.118460E 00	.715614E 01	.127665E 05	.104965E 08	.251057E-03	.223573E 03
64	.120442E 00	-.153186E 01	.131690E 05	.104978E 08	.251073E-03	.221453E 03
65	.122425E 00	.894621E 01	.134936E 05	.104992E 08	.251090E-03	.219399E 03
66	.124407E 00	.268836E 01	.138159E 05	.105005E 08	.251106E-03	.217413E 03
67	.126389E 00	.218212E 01	.141176E 05	.105018E 08	.251123E-03	.215465E 03
68	.128371E 00	.535449E 01	.145416E 05	.105029E 08	.251137E-03	.213551E 03
69	.130353E 00	.150429E 00	.148743E 05	.105040E 08	.251151E-03	.211702E 03
70	.132334E 00	.152686E 01	.152942E 05	.105051E 08	.251164E-03	.209864E 03
71	.134316E 00	-.134739E 01	.156750E 05	.105061E 08	.251177E-03	.208097E 03
72	.136297E 00	.924900E 00	.160904E 05	.105070E 08	.251189E-03	.206367E 03
73	.138279E 00	-.451444E 01	.164679E 05	.105080E 08	.251201E-03	.204649E 03
74	.140260E 00	-.134501E 01	.168383E 05	.105089E 08	.251213E-03	.202986E 03
75	.142241E 00	-.598995E 01	.172018E 05	.105099E 08	.251225E-03	.201347E 03
76	.144222E 00	-.422209E 01	.176165E 05	.105107E 08	.251236E-03	.199720E 03
77	.146203E 00	-.602355E 01	.183667E 05	.105110E 08	.251241E-03	.198109E 03
78	.148184E 00	-.487372E 01	.194157E 05	.105108E 08	.251241E-03	.196495E 03
79	.150165E 00	-.117142E 01	.210965E 05	.105097E 08	.251230E-03	.194846E 03
80	.152146E 00	-.168747E 01	.228442E 05	.105085E 08	.251218E-03	.193253E 03
81	.154127E 00	-.596696E 01	.247503E 05	.105070E 08	.251204E-03	.191624E 03
82	.156108E 00	-.267724E 01	.258183E 05	.105066E 08	.251201E-03	.190243E 03
83	.158090E 00	-.171632E 01	.262409E 05	.105071E 08	.251207E-03	.189013E 03
84	.160071E 00	-.147680E 01	.240766E 05	.105111E 08	.251251E-03	.188318E 03
85	.162052E 00	-.305337E 01	.207359E 05	.105163E 08	.251309E-03	.188219E 03
86	.164032E 00	.453725E 00	.149112E 05	.105185E 08	.251326E-03	.195727E 03

THICKNESS = .161162E 00

SPALL FRAGMENT = 2

VELOCITY OF MASS CENTER = .287187E 03 KINETIC E = .359703E 04

J	X (INCHES)	TRANSVERSE STRESS (PSI)	TANGENTIAL STRESS (PSI)	BULK MODULUS (PSI)	DENSITY	TEMPERATURE
88	.166515E 00	.930598E 01	.744571E 04	.105170E 08	.251295E-03	.210080E 03

THICKNESS = .502340E-03

SPALL FRAGMENT = 3

VELOCITY OF MASS CENTER = .748007E 03 KINETIC E = .366031E 06

J	X (INCHES)	TRANSVERSE STRESS (PSI)	TANGENTIAL STRESS (PSI)	BULK MODULUS (PSI)	DENSITY	TEMPERATURE
90	.171106E 00	-.832781E 00	.323876E 05	.105034E 08	.251174E-03	.182547E 03
91	.173088E 00	-.678475E 01	.248078E 05	.105169E 08	.251323E-03	.180676E 03
92	.175068E 00	.257191E 00	.215518E 05	.105237E 08	.251400E-03	.178719E 03
93	.177048E 00	.395986E 01	.162181E 05	.105331E 08	.251504E-03	.177430E 03
94	.179027E 00	-.803212E 01	.128974E 05	.105391E 08	.251572E-03	.176400E 03
95	.181005E 00	.748244E 01	.124377E 05	.105411E 08	.251594E-03	.175089E 03
96	.182983E 00	.269280E 01	.130922E 05	.105412E 08	.251597E-03	.173811E 03
97	.184961E 00	.417995E 01	.116058E 05	.105446E 08	.251635E-03	.172566E 03
98	.186939E 00	.602417E 01	.865734E 04	.105502E 08	.251697E-03	.171459E 03
99	.188916E 00	.157618E 01	.526292E 04	.105564E 08	.251766E-03	.170363E 03
100	.190893E 00	-.232862E 01	.245225E 04	.105615E 08	.251823E-03	.169512E 03
101	.192870E 00	-.242114E 01	-.512376E 04	.105735E 08	.251954E-03	.169182E 03
102	.194845E 00	-.260199E 01	-.597628E 04	.105759E 08	.251983E-03	.167859E 03
103	.196820E 00	-.505322E 00	-.165300E 05	.105924E 08	.252164E-03	.167546E 03
104	.198794E 00	-.308957E 01	-.193012E 05	.105974E 08	.252219E-03	.166773E 03

THICKNESS = .276875E-01

```
      SUBROUTINE PDATA (LINK)
      DIMENSION TPLOT(50)
      COMMON (USE MAIN)
      COMMON /PDAMP/ NTIME(50),KINET1(20),KINET2(20),SUMKIN(20),
     1CINS(20),JSS(40),DSTOP(20),NP,TDAMP,DFACT,KF,VCEN(20),NCOM(20)
      COMMON /EOSMAT/ GTEMP(1000)
      REAL KINET1,KINET2
      DATA LTP/0/
C
      GOTO (10,20,50,60,500),LINK
   10 READ(5,100) NP,(NTIME(I),I=1,NP)
      READ (5,100) LMAXP
      READ (5,160) (TPLOT(I),I=1,LMAXP)
      NT=1
      WRITE(6,110) (NTIME(I),I=1,NP)
      WRITE(6,150) (TPLOT(I),I=1,LMAXP)
      READ (5,120) TDAMP,DFACT
      WRITE (6,130) TDAMP,DFACT
      NP=1
      KMAX=0
      DO 11 I=1,20
      DSTOP(I)=0.0
      KINET1(I)=0.0
      KINET2(I)=0.0
   11 SUMKIN(I)=0.0
      NPLOT=3
C
      IF(NCYCLE .LE. 1)GOTO 45
   12 CALL SKIPFILE (NPLOT,1)
      READ (NPLOT) IFLAG
      IF(IFLAG .EQ. 99999)GOTO 14
      READ (NPLOT) IFLAG
      IF(IFLAG .NE. NCYCLE)GOTO 12
   14 CALL BACKFILE (NPLOT,1)
      GOTO 60
C
   20 CIN1=0.0
      CIN2=0.0
      CIN3=0.0
      CIN4=0.0
C     * * * * * *  COMPUTE KINETIC ENERGY (EACH REGION)  * * * * * * *
      DO 25 I=1,20
      NCOM(I)=0
   25 CONTINUE
C
      KF=1
      JK=1
      IFIRST=0
      CINS(1)=0.0
      VCEN(1)=0.0
      SMASS=0.0
      KEY=1
C
      DO 35 J=1,MAXZ
      IF(IVFLAG(J) .EQ. 0)GOTO 35
C                    HOT LIQUID REGION (VAPER-LIQUID)
      IF(IVFLAG(J) .EQ. 33) CIN1=CIN1+.125*DELTAM(J)*(U(J)+U(J+1))**2
C                    LIQUID REGION
      IF(IVFLAG(J) .EQ. 32) CIN2=CIN2+.125*DELTAM(J)*(U(J)+U(J+1))**2
C                    MELT REGION (LIQUID SOLID)
```

```
      IF(IVFLAG(J) .EQ. 31) CIN3=CIN3+.125*DELTAM(J)*(U(J)+U(J+1))**2
      IF(IVFLAG(J) .NE. 30)GOTO 35
      IF(IFIRST .EQ. 0) JSS(JK)=J
      IFIRST=1
C        COMPUTE KINETIC ENERGY OF EACH SOLID PIECE (FRAGMENT)
C        VELOCITY OF MASS CENTER OF EACH FRAGMENT
      CINS(KF)=CINS(KF)+.125*DELTAM(J)*(U(J)+U(J+1))**2
      SMASS=SMASS+DELTAM(J)
      VCEN(KF)=VCEN(KF)+.5*DELTAM(J)*(U(J)+U(J+1))
C                           ANY ZONE COMBINE
      IF(IBFLAG(J) .NE. 4)GOTO 28
      NCOM(KF+1)=1
      JSS(JK+1)=J
      JK=JK+2
      IFIRST=0
      GOTO 35
C
   28 IF(IBFLAG(J) .EQ. 2 )KEY=2
      GOTO (35,30),KEY
   30 VCEN(KF)=VCEN(KF)/SMASS
      IF(NCOM(KF+1) .EQ. 0)GOTO 31
      KF=KF+1
      VCEN(KF)=0.0
   31 JSS(JK+1)=J
      JK=JK+2
      KF=KF+1
      KEY=1
      IF(KF .GT. 20) GOTO 70
      CINS(KF)=0.0
      VCEN(KF)=0.0
      SMASS=0.0
      IFIRST=0
   35 CONTINUE
      VCEN(KF)=VCEN(KF)/SMASS
      JSS(JK+1)=MAXZ
C        SUM KINETIC ENERGY FOR KF FRAGMENTS
      VCENTR=VCEN(1)
      CIN4=0.
      DO 38 J=1,KF
      CIN4=CIN4+CINS(J)
   38 CONTINUE
C
      CINLS=CIN4
      CINL=CIN4+CIN3
      CINVL=CIN4+CIN3+CIN2
      CINV=CIN4+CIN3+CIN2+CIN1
C
      IFLAG=1
      WRITE(NPLOT) IFLAG
      WRITE(NPLOT) NCYCLE,TIME,VCENTR,KF,(CINS(I),I=1,KF)
C
      KMAX=MAX0(KMAX,KF)
      KF=KMAX
      CALL DAMP
C
   44 IF(NCYCLE .NE. NTIME(NP))GOTO 45
      NP=NP+1
      IFLAG=2
      WRITE(NPLOT) IFLAG
      WRITE(NPLOT) TIME,MAXZ,(X(J),S(J),P(J),SD(J),GTEMP(J),IVFLAG(J),
```

```
     1J=1,MAXZ)
  45 RETURN
C
  50 IFLAG=99999
     WRITE(NPLOT) IFLAG
     GOTO 45
C
  60 END FILE NPLOT
     GOTO 44
  70 WRITE(6,140) KF,NCYCLE
     IFLAG=99999
     WRITE(NPOLT) IFLAG
     CALL FORTRAN
C
 500 IF(LTP .EQ. 0)GOTO 510
     LTP=0
     IFLAG=2
     TIME=TIME-DTNP1
     WRITE(NPLOT) IFLAG
     WRITE(NPLOT) TIME,MAXZ,(X(J),S(J),P(J),SD(J),GTEMP(J),IVFLAG(J),
    1J=1,MAXZ)
     TIME=TIME+DTNP1
     GOTO 45
C
 510 IF(NT .GT. LMAXP)GOTO 45
     IF(TIME .LT. TPLOT(NT))GOTO 45
     DTNP1=TIME-TPLOT(NT)
     TIME=TIME-DTNP1
     LTP=1
     NT=NT+1
     GOTO 45
C
 100 FORMAT(16I5)
 110 FORMAT(5X,33HPLOTS AT THE FOLLOWING TIME STEPS/(5X,(16I5)))
 120 FORMAT (2E12.6)
 130 FORMAT (25H START DAMPING AFTER TIME,E12.6,5X,7HDFACT =,E12.6)
 140 FORMAT(' ENLARGE ARRAY CINS  K= ',I5,' TIME STEP = ',I5)
 150 FORMAT(5X,23HPLOTS AT FOLLOWING TIME/5X,(5E15.7))
 160 FORMAT(5E15.7)
     END
```

```
      SUBROUTINE DAMP
      COMMON (USE MAIN)
      COMMON /PDAMP/ NTIME(50),KINET1(20),KINET2(20),SUMKIN(20),
     1CINS(20),JSS(40),DSTOP(20),NP,TDAMP,DFACT,KF,VCEN(20),NCOM(20)
      REAL KINET1,KINET2
      DATA DCPSI/.0000145/
C
      DO 5 I=1,KF
      IF(NCOM(I) .EQ. 1)KINET2(I)=0.0
      KINET1(I)=KINET2(I)
      IF(NCOM(I) .EQ. 1)CINS(I)=0.0
      KINET2(I)=CINS(I)
    5 CONTINUE
C        CHECK FOR START OF DAMPING
      IF(TIME .LT. TDAMP)RETURN
C
      IF(KF .LT. 2)GOTO 12
      DO 10 I=2,KF
      IF(NCOM(I) .EQ. 1)VCEN(I)=0.0
      IF(VCEN(I).EQ. 0.0)GOTO 10
      IF(VCEN(I-1) .GT. VCEN(I)) RETURN
   10 CONTINUE
   12 KFINAL=1
C
      JK=1
      DO 30 I=1,KF
      IF(NCOM(I) .EQ. 1)GOTO 27
      IF(DSTOP(I).NE. 0.0)GOTO 53
      IF(KINET2(I) .GT. KINET1(I))GOTO 27
      SUMKIN(I)=SUMKIN(I)+CINS(I)
      JS=JSS(JK)
      JSN=JSS(JK+1)
      IF(JS .EQ. JSN)GOTO 53
      TRANS=0.0
      DO 52 J=JS,JSN
      TRANS=TRANS+ABS(S(J))
   52 CONTINUE
      TRANS=TRANS/FLOAT(JSN-JS+1)
      TRANS=TRANS*DCPSI
      IF(TRANS .LE. DFACT)GOTO 53
C         COMPUTE MOMENTUM OF FRAGMENT
      JS=JSS(JK)
      JSN=JSS(JK+1)
      IF(NCOM(I+1) .NE. 0)JSN=JSS(JK+3)
      DO 25 J=JS,JSN
      U(J)=VCEN(I)
   25 CONTINUE
      U(JSN+1)=VCEN(I)
   27 JK=JK+2
   30 CONTINUE
      RETURN
C
   53 DSTOP(I)=1.0
      IF(KFINAL .GE. KF)GOTO 55
      KFINAL=KFINAL+1
      GOTO 27
C
   55 WRITE(6,100) NCYCLE
      MAXCYL=NCYCLE
      TMAX=TIME
```

```
      NTIME(NP)=NCYCLE
      CALL EDIT
C
  100 FORMAT(1H1,10X,29HRUN SELF-TERMINATED TIME STEP,I5)
      END
```

```
      SUBROUTINE PETINP
C                                PETROS-3 INPUT
      COMMON (USE MAIN)
      COMMON /PCAMP/ NTIME(50),KINET1(20),KINET2(20),SUMKIN(20),
     1CINS(20),JSS(40),DSTOP(20),NP,TDAMP,DFACT,KF,VCEN(20),NCOM(20)
      COMMON /ECSMAT/ GTEMP(1000)
      DATA DCPSI/.0000145/CMTOIN/.3937/GCTOLB/.93502E-04/
C
      WRITE (6,100)
      JK=1
      DO 30 I=1,KF
      JS=JSS(JK)
      JSN=JSS(JK+1)
      VCENT=VCEN(I)*CMTOIN
      WRITE(6,110) I,VCENT,CINS(I)
      WRITE(6,130)
      IFIRST=1
      DO 20 J=JS,JSN
      TRANS=S(J)*DCPSI
      TANGS=-(P(J)-0.5*SD(J))*DCPSI
      TEMX=X(J)*CMTOIN
      BMS=(RHO(J)*C(J)**2)*DCPSI
      RHCP=RHO(J)*GCTCLB
      TEMF=32.0+(1.8*(GTEMP(J)-273.165))
      WRITE(6,140) J,TEMX,TRANS,TANGS,BMS,RHOP,TEMF
      IF(IFIRST .EQ. 1)THICK1=X(J)
      IFIRST=0
      THICK=(X(J)-THICK1)*CMTOIN
   20 CONTINUE
      JK=JK+2
      IF(JS .EQ. JSN) THICK=(X(JS)-X(JS-1))*CMTOIN
      WRITE(6,150) THICK
   30 CONTINUE
      RETURN
C
  100 FORMAT(1H1,59X,12HPETROS INPUT/)
  110 FORMAT(//55X,16HSPALL FRAGMENT =,I3/
     135X,25HVELOCITY OF MASS CENTER =,E12.6,1X,11HKINETIC E =E12.6/)
  130 FORMAT(/50X,10HTRANSVERSE,5X,10HTANGENTIAL,8X,4HBULK,10X,7HDENSITY
     1/30X,1HJ,4X,10HX (INCHES),4X,12HSTRESS (PSI),3X,12HSTRESS (PSI),3X
     2,13HMODULUS (PSI),19X,11HTEMPERATURE)
  140 FORMAT(28X,I3,6(3X,E12.6))
  150 FORMAT(/53X,11HTHICKNESS =,E12.6)
      END
```

APPENDIX B

BRL-RIP PLOTTING PROGRAM

The BRL-RIP plotting program is independent of the RIP program. It was written to monitor, by plotting, the output needed in coupling RIP to PETROS 3. The program makes use of the BRLESC FORTRAN Plotting Subroutines[16] which can easily be adapted to any other plotting system.

DESCRIPTION OF MAIN PROGRAM AND SUBROUTINES

The main program reads the plotting data tape and controls the flow of information. If the variable IFLAG equals one, data is read and stored in the plotting data arrays. If it equals two, data is read, converted to proper units and tangential stress is computed, then the program calls subroutine TPLOT. When IFLAG equals 99999, the program calls subroutine GRAPH.

If the number of cycles is greater than MAXA, subroutine GRAPH is called. If more cycles are needed, the following data arrays must be enlarged: TIM(MAXA), E(MAXA), VCEN(MAXA), and PKINE(N), where subscript N is equal to 20 times MAXA.

Subroutine TPLOT plots the profiles through the thickness, for the transverse stress, pressure, tangential stress and temperature. See Figures 6, 7, 8, and 9 for examples of the plotted output.

Subroutine GRAPH produces two graphs. The first is the kinetic energy versus time, which is useful for monitoring the solution, for the purpose of determining when to start damping and when to terminate the run. The second is the velocity of the mass center versus time. See Figures 10 and 11 for examples of the plotted output.

Subroutine PLOTD will plot data (drawline) for every zone in the mesh, but will skip any spall zone.

---

[16] *M. W. Coleman and J. V. Lanaham, BRLESC FORTRAN Plotting Subroutines," Aberdeen Research and Development Center, Technical Report No. 6, June 1970.*

Description of Variables

Name	Definition
B(1000)	Array used by the BRLESC FORTRAN Plotting Subroutines.
CINS(1000)	The array of numbers, corresponding to the kinetic energy of each fragment for a given time step.
DCPSI	Conversion constant (dynes/cm^2 to psi).
DX, DY	Spacing between increments in the X and Y directions used in labeling the axis.
GTEMP(1000)	Array of numbers corresponding to temperature profile through the thickness.
I	Index counter.
IFLAG	A flag. When it equals 1, program will read data for the timewise plots. When it equals 2, the program will read data for transverse stress, pressure, tangential stress, and temperature plots. When it equals 99999, the program will plot the timewise plots.
IVFLAG	See Reference 1, page 507.
J	Index counter.
KS	Number of spall fragments in the solid region.
LINK	Index used by a computed GOTO statement.
MAXA	Size of plotting arrays.
MAXJ	Number of zones (See Reference 1, page 507).
MJ	Index counter for number of cycles.
N	Index counter equal to the maximum MJ's.
NCYCLE	Counter on the number of cycles (see Reference 1, page 506).
NPLOT	Magnetic plotting tape input unit number.
PJ(1000)	Array of numbers corresponding to pressure profile through the thickness.

[1] *R. H. Fisher, G. A. Lane and R. A. Cecil, "RIP, A One-Dimensional Material Response Code - User's Guide," Systems, Science and Software, Report 3SR-751-I, September 1972.*

PKINE(20000)	The array of numbers, corresponding to kinetic energy of the fragments in the solid region.
SDJ(1000)	The array of numbers, corresponding to stress deviator through the thickness.
SJ(1000)	The array of numbers, corresponding to stress through the thickness.
STEP(2)	Array corresponding to label of current time.
SYM_i i = 1, 5	Arrays corresponding to labels on the axes.
TEMP	Temporary name.
TIM(1000)	The array of numbers, corresponding to time history.
TIME	Current value of time.
VCEN(1000)	The array of numbers, corresponding to the velocity of mass center of the largest remaining solid region.
XBAR, YBAR	Board coordinates of a point on the plotting surface.
XJ(1000)	The array of numbers, corresponding to the spatial coordinates.
XL	Length of x-axis in inches.
XMAX	Maximum x-coordinate.
XMIN	Minimum x-coordinate.
XPAGE	Plotting page length.
XS, YS	Scales in the X and Y directions.
XSCALE	Scale in the X direction.
X_1, X_2	Plotting arrays for the X and Y directions.

```
C         BRL-RIP PLOTTING PROGRAM (BRLESC FORTRAN PLOTTING SUBROUTINES)
      COMMON TIM(1C00),GTEMP(1000),IVFLAG(1000),VCEN(1000),
     1XJ(1000),SJ(1000),PJ(1000),SDJ(1000),MAXZ,MJ,NCYCLE,TIME
      COMMON KS,MAXA,CINS(20),PKINE(20000)
      DATA DCPSI/.CC00145/
*         MVPRTO(01K00)
*         SUBR(PLTCCB=01400)
C
      NPLOT=3
      REWIND NPLOT
      MJ=0
      MAXA=1000
   10 READ(NPLOT) IFLAG
      IF(IFLAG .EQ. 99999)GOTO 40
      GOTO(20,25),IFLAG
C
   20 MJ=MJ+1
      READ(NPLOT) NCYCLE,TIM(MJ),VCEN(MJ),KS,(CINS(I),I=1,KS)
      IF(NCYCLE .GE. MAXA) CALL GRAPH
C
      TEMP=0.0
      DO 22 I=1,20
      J=MJ+MAXA*(I-1)
      TEMP=TEMP+CINS(I)
      PKINE(J)=TEMP
   22 CONTINUE
      GOTO 10
C
   25 READ (NPLOT) TIME,MAXZ,(XJ(I),SJ(I),PJ(I),SDJ(I),GTEMP(I),
     1IVFLAG(I),I=1,MAXZ)
      TIME=TIM(MJ)
      DO 30 I=1,MAXZ
      SJ(I)=SJ(I)*DCPSI
      PJ(I)=PJ(I)*DCPSI
      SDJ(I)=SDJ(I)*DCPSI
      SDJ(I)=PJ(I)-0.5*SDJ(I)
   30 CONTINUE
      CALL TPLOT
      GOTO 10
C
   40 CALL GRAPH
      CALL EXIT
      END
```

```
      SUBROUTINE TPLOT                                                  ****
      DIMENSION B(1000),SYM1(3),SYM2(3),SYM3(2),STEP(2),SYM4(3),SYM5(2) TPLO
      COMMON (USE MAIN)                                                 TPLO
      COMMON /PLOT/B                                                    TPLO
      DATA (SYM1(I),I=1,3)/10HSPACIAL CO,10HORDINATE (,4HCM)>/,         TPLO
     1     (SYM2(I),I=1,3)/10HTRANSVERSE,10H STRESS (P,4HSI)>/,         TPLO
     2     (SYM3(I),I=1,2)/10HPRESSURE (,5HPSI)>/                       TPLO
     3     (SYM4(I),I=1,3)/10HTANGENTIAL,10H STRESS (P,4HSI)>/,         TPLO
     4     (SYM5(I),I=1,2)/10HTEMPERATUR,2HE>/                          TPLO
      XL=7.0                                                            TPLO
      YL=6.0                                                            TPLO
      LINK=1                                                            TPLO
C                                                                       TPLO
      XPAGE=12.0                                                        TPLO
      CALL PLTCCB (XPAGE,1,B(1),B(1000))                                TPLO
      N=MAXZ                                                            TPLO
C     ----------------------- GRAPH ONE ---------------------------------TPLO
      XBAR=3.0                                                          TPLO
      YBAR=2.0                                                          TPLO
      CALL FIXSCA (XJ(1),N,XL,XS,XMIN,XMAX,DX)                          TPLO
      CALL FIXSCA (SJ(1),N,YL,YS,YMIN,YMAX,DY)                          TPLO
      CALL PLTCCS (XBAR,YBAR,XMIN,YMIN,XS,YS)                           TPLO
      CALL PLTCCA (DX,DY,XMIN,XMAX,YMIN,YMAX,4)                         TPLO
      CALL PLOTD (XJ,SJ)                                                TPLO
      CALL LABELA (DX,DY,XMIN,XMAX,YMIN,YMAX,1.0,1.0)                   TPLO
      CALL PLTCCS (XBAR,YBAR,0.0,0.0,1.0,1.0)                           TPLO
      CALL PLTCCT (.1,SYM1(1),0.0,1.0,2.3,-0.6)                         TPLO
      CALL PLTCCT (.1,7HS=P+SD>,1.0,0.0,-1.4,2.7)                       TPLO
      CALL PLTCCT (.1,SYM2(1),1.0,0.0,-1.2,1.8)                         TPLO
C     - - - - - - - - - - - - - - - - - - - - - - - - - - - - - - - - - TPLO
   50 CALL PLTCCT (.1,6HCYCLE>,0.0,1.0,0.0,-1.0)                        TPLO
      ENCODE (6,100,STEP) NCYCLE                                        TPLO
      CALL PLTCCT (.1,STEP(1),0.0,1.0,0.6,-1.0)                         TPLO
      CALL PLTCCT (.1,6HTIME=>,0.0,1.0,0.0,-1.2)                        TPLO
      ENCODE(12,110,STEP) TIME                                          TPLO
      CALL PLTCCT (.1,STEP(1),0.0,1.0,0.6,-1.2)                         TPLO
      GOTO(55,60,65,70),LINK                                            TPLO
C     ----------------------- GRAPH TWO ---------------------------------TPLO
   55 YBAR=12.0                                                         TPLO
      CALL FIXSCA (PJ(1),N,YL,YS,YMIN,YMAX,DY)                          TPLO
      CALL PLTCCS (XBAR,YBAR,XMIN,YMIN,XS,YS)                           TPLO
      CALL PLTCCA (DX,DY,XMIN,XMAX,YMIN,YMAX,4)                         TPLO
      CALL PLOTO (XJ,PJ)                                                TPLO
      CALL LABELA (DX,DY,XMIN,XMAX,YMIN,YMAX,1.0,1.0)                   TPLO
      CALL PLTCCS (XBAR,YBAR,0.0,0.0,1.0,1.0)                           TPLO
      CALL PLTCCT (.1,SYM1(1),0.0,1.0,2.3,-0.6)                         TPLO
      CALL PLTCCT (.1,SYM3(1),1.0,0.0,-1.2,2.3)                         TPLO
      LINK=2                                                            TPLO
      GOTO 50                                                           TPLO
C     ----------------------- GRAPH THREE -------------------------------TPLO
   60 YBAR=22.0                                                         TPLO
      CALL FIXSCA (SDJ(1),N,YL,YS,YMIN,YMAX,DY)                         TPLO
      CALL PLTCCS (XBAR,YBAR,XMIN,YMIN,XS,YS)                           TPLO
      CALL PLTCCA (DX,OY,XMIN,XMAX,YMIN,YMAX,4)                         TPLO
      CALL PLOTO (XJ,SOJ)                                               TPLO
      CALL LABELA (OX,OY,XMIN,XMAX,YMIN,YMAX,1.0,1.0)                   TPLO
      CALL PLTCCS (XBAR,YBAR,0.0,0.0,1.0,1.0)                           TPLO
      CALL PLTCCT (.1,SYM1(1),0.0,1.0,2.3,-0.6)                         TPLO
      CALL PLTCCT (.1,10HS=P-.5*SD>,1.0,0.0,-1.4,2.5)                   TPLO
      CALL PLTCCT (.1,SYM4(1),1.0,0.0,-1.2,1.8)                         TPLO
```

```
      LINK=3
      GOTO 50
C     ------------------------ GRAPH FOUR ------------------------------
   65 CALL PLTCCP
      XBAR=3.0
      YBAR=2.0
      CALL FIXSCA (GTEMP(1),N,YL,YS,YMIN,YMAX,DY)
      CALL PLTCCS (XBAR,YBAR,XMIN,YMIN,XS,YS)
      CALL PLTCCA (DX,DY,XMIN,XMAX,YMIN,YMAX,4)
      CALL PLOTD (XJ,GTEMP)
      CALL LABELA (DX,DY,XMIN,XMAX,YMIN,YMAX,1.0,1.0)
      CALL PLTCCS (XBAR,YBAR,0.0,0.0,1.0,1.0)
      CALL PLTCCT (.1,SYM1(1),0.0,1.0,2.3,-0.6)
      CALL PLTCCT (.1,SYM5(1),1.0,0.0,-1.0,2.5)
      LINK=4
      GOTO 50
   70 CALL PLTCCP
      RETURN
C
  100 FORMAT(I4,2H >)
  110 FORMAT(E12.7,2H >)
      END
```

```
      SUBROUTINE GRAPH                                                  ****
      DIMENSION B(1000),SYM1(2),SYM2(2),SYM3(4)                         GRAP
      COMMON (USE MAIN)                                                 GRAP
      COMMON /PLOT/B                                                    GRAP
      DATA (SYM1(I),I=1,2)/10HTIME (NANO,9HSECONDS)>/,                  GRAP
     1     (SYM2(I),I=1,2)/10HKINETIC EN,5HERGY>/                       GRAP
      DATA (SYM3(I),I=1,4)/10HVELOCITY O,10HF MASS CEN,10HTER (CM/SE,3HCGRAP
     1)>/                                                               GRAP
C                                                                       GRAP
      N=MJ                                                              GRAP
      XL=7.0                                                            GRAP
      YL=6.0                                                            GRAP
      XSCALE=1.0E9                                                      GRAP
C     ------------------------ GRAPH ONE -------------------------------GRAP
      XBAR=3.0                                                          GRAP
      YBAR=2.0                                                          GRAP
      CALL FIXSCA (TIM(1),N,XL,XS,XMIN,XMAX,DX)                         GRAP
      CALL PLTCCS (XBAR,YBAR,0.0,0.0,1.0,1.0)                           GRAP
      CALL PLTCCT (.1,SYM1(1),0.0,1.0,2.5,-0.6)                         GRAP
      CALL PLTCCT (.1,SYM2(1),1.0,0.0,-1.2,2.3)                         GRAP
      DO 10 I=1,KS                                                      GRAP
      J=1+MAXA*(I-1)                                                    GRAP
      IF(J .EQ. 1) CALL FIXSCA (PKINE(J),N,YL,YS,YMIN,YMAX,DY)          GRAP
      CALL CONSCA (PKINE(J),N,YL,YS,YMIN,YMAX,DY)                       GRAP
   10 CONTINUE                                                          GRAP
C                                                                       GRAP
      CALL PLTCCS (XBAR,YBAR,XMIN,YMIN,XS,YS)                           GRAP
      CALL PLTCCA (DX,DY,XMIN,XMAX,YMIN,YMAX,4)                         GRAP
      DO 20 I=1,KS                                                      GRAP
      J=1+MAXA*(I-1)                                                    GRAP
      CALL PLTCCD (1,0,TIM(1),PKINE(J),N,0,XMIN,XMAX,YMIN,YMAX)         GRAP
   20 CONTINUE                                                          GRAP
      CALL LABELA (DX,DY,XMIN,XMAX,YMIN,YMAX,XSCALE,1.0)                GRAP
C     ------------------------ GRAPH TWO -------------------------------GRAP
      YBAR=12.0                                                         GRAP
      CALL PLTCCS (XBAR,YBAR,0.0,0.0,1.0,1.0)                           GRAP
      CALL PLTCCT (.1,SYM1(1),0.0,1.0,2.5,-0.6)                         GRAP
      CALL PLTCCT (.1,SYM3(1),1.0,0.0,-1.2,1.3)                         GRAP
      CALL FIXSCA ( VCEN(1),N,YL,YS,YMIN,YMAX,DY)                       GRAP
      CALL PLTCCS (XBAR,YBAR,XMIN,YMIN,XS,YS)                           GRAP
      CALL PLTCCA (DX,DY,XMIN,XMAX,YMIN,YMAX,4)                         GRAP
      CALL PLTCCD (1,0,TIM(1),VCEN(1),N)                                GRAP
      CALL LABELA (DX,DY,XMIN,XMAX,YMIN,YMAX,XSCALE,1.0)                GRAP
      CALL PLTCCP                                                       GRAP
      RETURN                                                            GRAP
      END                                                               GRAP
```

```
      SUBROUTINE PLOTD (Y1,Y2)
      COMMON (USE MAIN)
      DIMENSION X1(1000),X2(1000),Y1(1),Y2(1)
C
      K=0
      DO 5 J=1,MAXZ
      IF(IVFLAG(J) .EQ. 0)GOTO 10
      K=K+1
      X1(K)=Y1(J)
      X2(K)=Y2(J)
    5 CONTINUE
   10 CALL PLTCCD (1,0,X1(1),X2(1),K)
      K=0
      IF(J .GE. MAXZ) RETURN
      GOTO 5
      END
```

APPENDIX C

CODING CHANGES TO PETROS 3

Two changes were required in the BRL version of PETROS 3 for it to be able to accept RIP data. The first change was the alteration of the material properties subroutine, MATPRO, to permit the introduction of variable material properties (E, ν, ρ, σ_o) for each Gaussian layer through the thickness.

The second change was made in order to have an initial stress distribution through the thickness (see Figure 8) rather than a zero stress state at the start of the calculation. The subroutine ISTRES reads spatial coordinates and tangential stress (see Table A-1). After all cards are read, linear interpolation through the thickness for values of tangential stress at each Gauss point is performed. Then the initial strain energy is determined. This subroutine is called from within subroutine STEP1, following card STP11020, page 349, Reference 5, by the statement CALL ISTRES; it is only called at time step zero.

The following is a FORTRAN listing of the two subroutines as they are used in the BRL version of PETROS 3.

```
      SUBROUTINE MATPRO
C     EVALUATE MATERIAL PROPERTIES
C     THIS VERSION IS FOR RIP MATERIAL PROPERTIES
C
      COMMON (USE MAIN)
      COMMON /CONTN2/          EE1(4),EE2(4),         HNU1(4),HNU2(4),
     1CONSTZ(4),CONST1(4),CONST2(4),EXPONZ(4),EXPON1(4),EXPON2(4),
     2         RHO1(4),RHO2(4),SIG1DZ(4,5),SIG1D1(4,5),SIG1D2(4,5),
     3EPS1DZ(4,5),EPS1D1(4,5),EPS1D2(4,5),COEFFZ(4,5),SIGMAZ(4,5),
     4THIKNS(4,14,21),CENTRZ(4,14,21),ALPHAZ(4),EEZ(6,6),HNUZ(6,6),
     5RHOZ(6,6)
      DIMENSION SIG1DT( 5),EPS1DT( 5),EEET( 6)
C
      IF(QMATPR) GO TO 103
      WRITE(NWRITE,10)
   10 FORMAT('1 SUBROUTINE MATPRO RIP MATERIAL PROPERTIES')
   11 FORMAT(5E15.6)
      DO 101 ILAY=1,NLAYER
      READ (NREAD,11) CONSTZ(ILAY),EXPONZ(ILAY),ALPHAZ(ILAY)
      WRITE (NWRITE,11) CONSTZ(ILAY),EXPONZ(ILAY),ALPHAZ(ILAY)
      NGAUSL=NGAUSS(ILAY)
      DO 101 IGAU  =1,NGAUSL
      READ (NREAD,11) RHOZ(ILAY,IGAU  ),EEZ(ILAY,IGAU  ),
     1HNUZ(ILAY,IGAU  ),SIG1DZ(ILAY,IGAU  )
      WRITE (NWRITE,11) RHOZ(ILAY,IGAU  ),EEZ(ILAY,IGAU  ),
     1HNUZ(ILAY,IGAU  ),SIG1DZ(ILAY,IGAU  )
  101 CONTINUE
      QMATPR=.TRUE.
C
  103 RHO=RHOZ(ILAYER,IGAUSS)
      EE=EEZ(ILAYER,IGAUSS)
      HNU=HNUZ(ILAYER,IGAUSS)
      CONST=CONSTZ(ILAYER)
      EXPON=EXPONZ(ILAYER)
      ALPHA=ALPHAZ(ILAYER)
C
      NSBL=NSUBL(ILAYER)
      DO 100 ISUBL=1,NSBL
      COEFF(ISUBL)=1.0
      SIGMA(ISUBL)=SIG1DZ(ILAYER,IGAUSS)
  100 CONTINUE
      RETURN
      END
```

```
      SUBROUTINE ISTRES
      COMMON (USE MAIN)
      COMMON /CONTN3/ TAU11(14,21, 6),TAU12(14,21, 6),TAU22(14,21, 6)
      DIMENSION X(100),STRES(100)
C
      IF(QSTRES) GOTO 30
      QSTRES=.TRUE.
C        READ INITIAL STRESS DATA FROM CARDS
      READ (5,500) N
      DO 5 I=1,N
      READ (NREAD,510) X(I),STRES(I),DUM
      X(I)=X(I)-X(1)
    5 CONTINUE
      HALF=.5*X(N)
      NN=N-1
      X(1)=HALF
      X(N)=-HALF
      DO 10 I=2,NN
      X(I)=HALF-X(I)
   10 CONTINUE
C
      WRITE(6,520)
      DO 20 I=1,N
      WRITE(6,530) X(I),STRES(I)
   20 CONTINUE
C
   30 IF(Z.LT.X(N) .OR. Z.GT.X(1))GOTO 50
      DO 40 I=2,N
      IF(Z .GE. X(I))GOTO 45
   40 CONTINUE
   45 IM=I-1
      FSTRE=STRES(IM)+(Z-X(IM))*(STRES(I)-STRES(IM))/(X(I)-X(IM))
      GOTO 55
   50 FSTRE=0.0
   55 DO 151 LA=1,2
      DO 151 LB=1,2
      TS(LA,LB) = 0.0
  151 G(LA,LB)=A(LA,LB)-2.*Z*B(LA,LB)
      GO=G(1,1)*G(2,2)-G(1,2)**2
      SRG=SQRT(GO)
C
      NSBL=NSUBL(ILAYER)
      DO 160 ISB=1,NSBL
      IZ=IZ+1
      TAU11(I1,I2,IZ)=FSTRE/G(1,1)
      TAU12(I1,I2,IZ)=0.0
      TAU22(I1,I2,IZ)=FSTRE/G(2,2)
      TAUSBL(1,1)=TAU11(I1,I2,IZ)
      TAUSBL(1,2)=TAU12(I1,I2,IZ)
      TAUSBL(2,2)=TAU22(I1,I2,IZ)
      TAUSBL(2,1)=TAUSBL(1,2)
C
      DO 155 LA=1,2
      DO 155 LB=1,2
      TM(LA,LB)=TAUSBL(LA,1)*G(1,LB)+TAUSBL(LA,2)*G(2,LB)
  155 TS(LA,LB)=TS(LA,LB) + COEFF(ISB)*TM(LA,LB)
  160 CONTINUE
C           STRAIN ENERGY
      NGAUSL=NGAUSS(ILAYER)
```

```
      PAR=THICKN*.5*WEIGHT(IGAUSS,NGAUSL)
      CB = PAR*CA/EE
      IF(I1.EQ.ISTR1 .OR. I1.EQ.ISTR3)SRG=0.5*SRG
      IF(I2.EQ.ISTR2 .OR. I2.EQ.ISTR4)SRG=0.5*SRG
      STREN=STREN+((TS(1,1)+TS(2,2))**2-2.*(1.0+HNU)*(TS(1,1)*TS(2,2)
     1       - TS(1,2)*TS(2,1)))*SRG*CB
      RETURN
C
  500 FORMAT(I5)
  510 FORMAT(3E15.6)
  520 FORMAT(1H1,52X,28HSTRESS THROUGH THE THICKNESS/70X,10HTANGENTAIL/
     153X,9HTHICKNESS,10X,6HSTRESS)
  530 FORMAT(51X,E13.6,4X,E13.6)
      END
```

APPENDIX D

TEMPERATURE VARIATION DURING STRUCTURAL RESPONSE

As noted previously, the PETROS 3 calculations were made on the premise that the initial temperature distribution through the thickness of the residual plate was frozen for the duration of the structural response prediction (5,520 microseconds). Although this duration is quite brief, it was felt desirable to determine the extent of temperature redistribution which could occur during this period. Consequently, a heat transfer problem for the residual aluminum plate was formulated. By assuming that the edges of the plate were insulated, the problem is reduced to one spatial dimension: the through-thickness direction. On the front and back faces of the residual plate the boundary conditions were taken to be the radiation-type. The solution to this intial-value problem was obtained by using the CINDA code[17]. The results, consisting of a comparison of temperature distributions at the initial and final times of the PETROS 3 calculation, are shown in Figure D-1. The abscissa in this plot represents the distance from the front face of the residual plate. It may be seen that there is an appreciable change in temperature during the plate response, especially in the neighborhood of the front face.

It would obviously be desirable to take this temperature variation into account in future structural response calculations of this type. This may readily be accomplished if one is willing to make the plausible assumption that thermomechanical coupling can be neglected. The CINDA code could be employed to obtain the transient temperature distributions (at frequent time intervals) and storage of these data on a magnetic tape could be read by the PETROS 3 code as the structural response solution is marched out in time.

Recalling that the PETROS 3 calculations were made using both cold and heated material properties in an effort to bound the true solution, the latter case corresponding to instant degradation of material strength with temperature, raises another question as to the proper modeling of the physical event when heat transfer is considered. That is, should the instantaneous recovery of material strength be allowed in those portions of the structure which are cooking? Full recovery of strength does not occur in metals which are subjected to elevated temperatures for long soak times and then slowly permitted to cool. While the response under consideration certainly does not allow time for annealing, it would be more consistent with the objective of predicting a bound on the response in the heated material case if one allowed no recovery of material strength following the maximum temperature excursion.

---

[17] *J. D. Gask, "Chrysler Improved Numerical Differencing Analyser for Third Generation Computers," Chrysler Corporation Space Division, TN-AP-67-287, October 1967.*

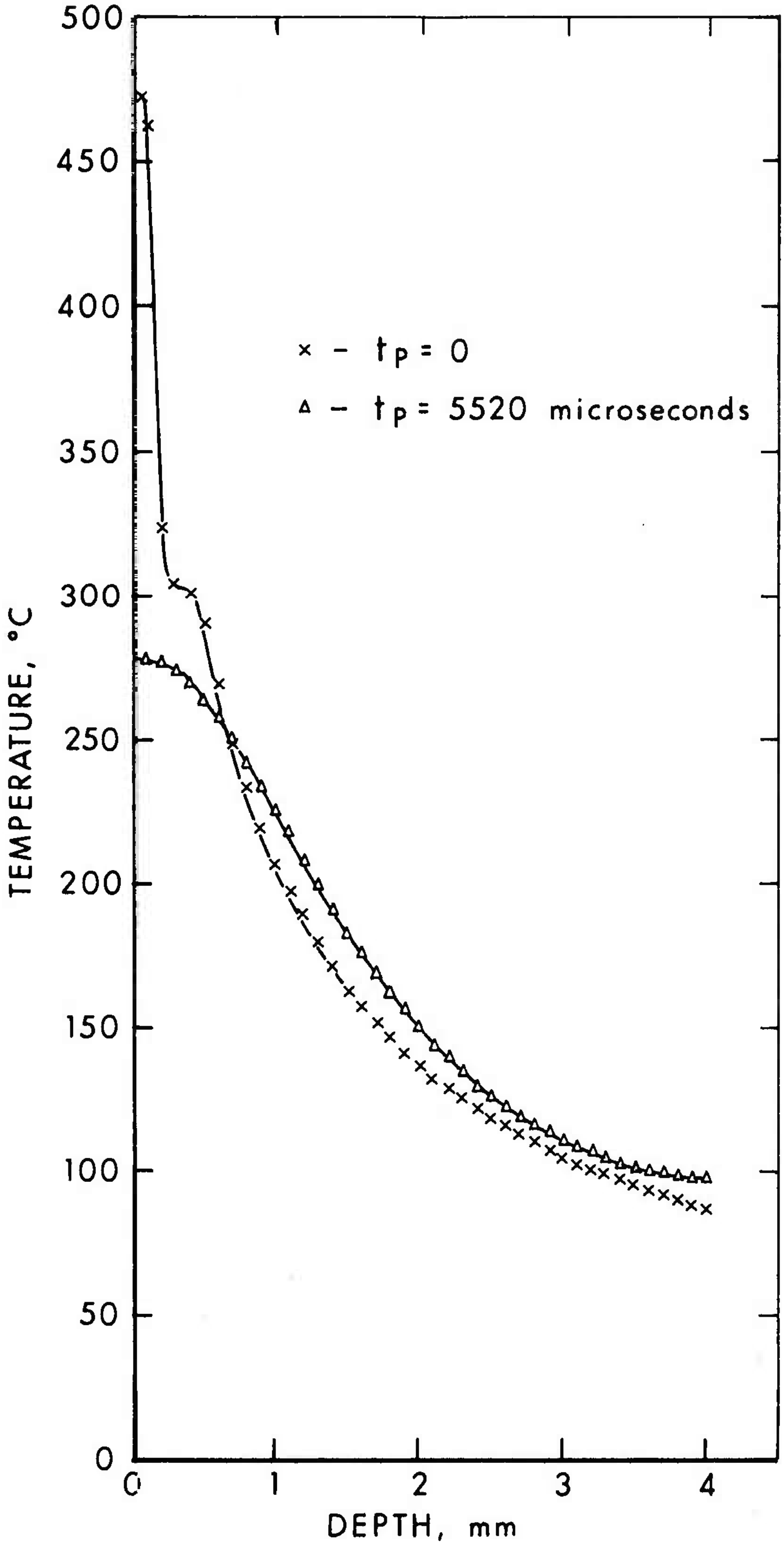

Figure D-1. Temperature Profiles at Beginning and End of Structural Response

DISTRIBUTION LIST

No. of Copies	Organization
12	Commander Defense Documentation Center ATTN: DDC-TCA Cameron Station Alexandria, VA 22314
1	Director Defense Advanced Research Projects Agency 1400 Wilson Boulevard Arlington, VA 22209
1	Director Weapons Systems Evaluation Group, ODDR&E ATTN: CPT Donald E. McCoy Washington, DC 20305
1	Assistant to the Secretary of Defense (Atomic Energy) ATTN: Document Control Washington, DC 20301
1	Office Secretary of Defense Office DDR&E ATTN: Mr. J. Persh, Staff Specialist Materials and Structures Washington, DC 20301
5	Director Defense Nuclear Agency ATTN: Mr. J. F. Moulton, SPAS Dr. LaVier, STVL Cdr Alderson, RATN Dr. E. Sevin, SPSS Dr. M. C. Atkins, DDST Washington, DC 20305
4	Director Defense Nuclear Agency ATTN: SPTL Tech Lib (2 cys) APSI (ARCHIVES) STSP Washington, DC 20305
1	Commander Field Command Defense Nuclear Agency ATTN: Tech Lib, FCWS-SC Kirtland AFB, NM 87115
1	Chief Las Vegas Liaison Office Field Command TD, DNA P.O. Box 2702 ATTN: Document Control Las Vegas, NV 89104
1	DNA Information and Analysis Center TEMPO, General Electric Co. Center for Advanced Studies ATTN: DASIAC 816 State Street Santa Barbara, CA 93102
1	Director Defense Communications Agency ATTN: NMCSSC (Code 510) Washington, DC 20305
2	Director Defense Intelligence Agency ATTN: DT-1C, Dr. J. Vorona DT-2 Washington, DC 20301
3	Director Institute for Defense Analyses ATTN: Dr. J. Menkes Dr. J. Bengston Tech Info Ofc 400 Army-Navy Drive Arlington, VA 22202
2	Chairman Joint Chiefs of Staff ATTN: J-3, Operations J-5, Plans & Policy (R&D Division) Washington, DC 20301

DISTRIBUTION LIST

No. of Copies	Organization
1	Commander US Army Materiel Development and Readiness Command ATTN: DRCDMA-ST 5001 Eisenhower Avenue Alexandria, VA 22333
1	Commander US Army Materiel Development and Readiness Command ATTN: DRCPM-CS 5001 Eisenhower Avenue Alexandria, VA 22333
1	Commander US Army Aviation Systems Command ATTN: DRSAV-E 12th and Spruce Streets St. Louis, MO 63166
1	Director US Army Air Mobility Research and Development Laboratory Ames Research Center Moffett Field, CA 94035
1	Commander US Army Electronics Command ATTN: DRSEL-RD Fort Monmouth, NJ 07703
3	Commander US Army Missile Research and Development Command ATTN: MIRADCOM-R MIRADCOM-AOM, Library MIRADCOM-RSS, Mr. B. Cobb Redstone Arsenal, AL 35809
2	Commander US Army Missile Research and Development Command ATTN: MIRADCOM-RX, Mr. W. Thomas MIRADCOM-RR, Mr. L. Lively Redstone Arsenal, AL 35809
1	Commander US Army Tank Automotive Development Command ATTN: DRDTA-RWL Warren, MI 48090
2	Commander US Army Mobility Equipment Research & Development Command ATTN: Tech Docu Cen, Bldg. 315 DRSME-RZT Fort Belvoir, VA 22060
1	Commander US Army Armament Materiel Readiness Command ATTN: Technical Library Rock Island, IL 61202
1	Commander US Army Frankford Arsenal ATTN: SARFA-L6100, Dr. P. Flynn Philadelphia, PA 19137
4	Commander US Army Armament R&D Command ATTN: DRDAR-LC, Dr. J. Frasier DRDAR-LCF, Mr. G. Demitrack DRDAR-LCN, Mr. W. Benson DRDAR-LCN, Mr. P. Angelotti Dover, NJ 07801
1	Commander US Army Watervliet Arsenal Watervliet, NY 12189

DISTRIBUTION LIST

No. of Copies	Organization
9	Commander US Army Harry Diamond Labs ATTN: DRXDO-TI Dr. R. Oswald Mr. F. N. Wimenitz Mr. L. Belliveau Mr. J. Corrigan Mr. J. Gwaltney Mr. E. J. Gaul Mr. D. Schallhorn DRXDO-RBH Mr. P. A. Caldwell 2800 Powder Mill Road Adelphi, MD 20783
3	Commander US Army Materials and Mechanics Research Center ATTN: DRXMR-ATL DRXMR-ED Mr. R. Shea DRXRD, J. Dignam Watertown, MA 02172
1	Commander US Army Natick Research and Development Command ATTN: DRXRE, Dr. D. Sieling Natick, MA 01762
1	Commander US Army Foreign Science and Technology Center ATTN: Rsch & Data Branch Federal Office Building 220 - 7th Street, NE Charlottesville, VA 22901
2	Commander US Army Nuclear Agency ATTN: ACTA-NAW Technical Library Fort Bliss, TX 79916

No. of Copies	Organization
1	Commander US Army TRADOC Systems Analysis Activity ATTN: ATAA-SA White Sands Missile Range NM 88002
1	Interservice Nuclear Weapons School ATTN: Technical Library Kirtland AFB, NM 87115
1	Director DARCOM Field Safety Activity ATTN: DRXOS-ES Charlestown, IN 47111
1	Director DARCOM, ITC ATTN: Dr. Chiang Red River Depot Texarkana, TX 75501
1	Director US Army Ballistic Missile Defense Program Office ATTN: J. Shea 5001 Eisenhower Avenue Alexandria, VA 22333
6	Director US Army Ballistic Missile Defense Advanced Technology Center ATTN: M. Whitfield J. Davidson M. Capps N. J. Hurst J. G. Bauxbaum J. Veeneman P.O. Box 1500, West Station Huntsville, AL 35807

DISTRIBUTION LIST

No. of Copies	Organization
1	Director US Army Engineer School Fort Belvoir, VA 22060
2	HQDA (DAMA-AR; NCL Div) Washington, DC 20310
1	Commander US Army Research Office P.O. Box 12211 Research Triangle Park NC 27709
1	Director US Army Engineer Waterways Experiment Station P.O. Box 631 Vicksburg, MS 39180
1	US Army Eng Div ATTN: Mr. Char P.O. Box 1600 Huntsville, AL 35809
1	US Army Corps of Engineers Huntsville Division ATTN: Dick Bradshaw HNDED-SR P.O. Box 1600, West Station Huntsville, AL 35807
2	Director Joint Strategic Target Planning Staff ATTN: JLTW JPTP Offutt AFB Omaha, NB 68113
4	Chief of Naval Operations ATTN: OP-03EG OP-97 OP-754 OP-985FZ Department of the Navy Washington, DC 20350
1	Assistant Secretary of the Navy (Research & Development) Navy Department Washington, DC 20350
1	Chief of Naval Material ATTN: Code 418, Dr. T. Quinn Navy Department Arlington, VA 22217
4	Commander David W. Taylor Naval Ship Research & Development Center ATTN: Dr. W. W. Murray, Code 17 Mr. R. Jones, Code 1725 Dr. G. Everstine, Code 1844 Dr. B. Whang, Code 174.4 Bethesda, MD 20084
2	Commander US Naval Surface Weapons Center ATTN: Mr. J. C. Talley Dr. W. Soper Dahlgren, VA 22448
4	Commander US Naval Surface Weapons Center ATTN: Dr. Leon Schindel Dr. Victor Dawson Dr. P. Huang Code 121, Navy Nuclear Programs Office Silver Spring, MD 20910
1	Commander Naval Surface Weapons Center ATTN: Code 241 (Mr. Proctor) Silver Spring, MD 20910
1	Commander US Naval Weapons Center ATTN: Code 6031 Dr. W. Stronge China Lake, CA 93555

DISTRIBUTION LIST

No. of Copies	Organization
1	Commander US Naval Ship Research and Development Center Facility ATTN: Mr. Lowell T. Butt Underwater Explosions Research Division Portsmouth, VA 23709
1	Commander US Naval Weapons Evaluation Facility ATTN: Document Control Kirtland AFB Albuquerque, NM 87117
1	Commander Naval Civil Engineering Lab ATTN: J. Tancreto Port Hueneme, CA 93041
1	Commander US Naval Research Laboratory ATTN: Code 2027, Tech Lib Washington, DC 20375
2	Superintendent US Naval Postgraduate School ATTN: Tech Reports Section Code 57, Prof R. Ball Monterey, CA 93940
1	HQ USAF (AFNIE-CA) Washington, DC 20330
4	HQ USAF (AFRDQ; AFRDOSM; AFRDPM; AFRD) Washington, DC 20330
1	AFSC (DSCPSL) Andrews AFB Washington, DC 20331
2	AFATL (ATRD, R. Brandt) Eglin AFB, FL 32542

No. of Copies	Organization
1	ADTC (ADBPS-12) Eglin AFB, FL 32542
1	USAFTAWC (OA) Eglin AFB, FL 32542
3	AFWL (WLA; WLD; WLRP, LTC H. C. McClammy) Kirtland AFB, NM 87117
4	AFWL (SYT, MAJ W. A. Whitaker; SRR; SUL; SR) Kirtland AFB, NM 87117
1	AFFDL (FDTR, Dr. R. M. Bader) Wright-Patterson AFB, OH 45433
4	AFML (MAMD, Dr. T. Nicholas; MAS; MANC, Mr. D. Schmidt; MAX, Dr. A. M. Lovelace) Wright-Patterson AFB, OH 45433
2	FTD (TDPTN; TDFBD, J. D. Pumphrey) Wright-Patterson AFB, OH 45433
1	Headquarters Energy Research and Development Administration Department of Military Applications Washington, DC 20545
2	Headquarters National Aeronautics and Space Administration ATTN: Mr. J. Enders, Code RAO Mr. K. Strass, Code RY Washington, DC 20546

DISTRIBUTION LIST

No. of Copies	Organization
2	National Aeronautics and Space Administration Aerospace Safety Research and Data Institute ATTN: Mr. S. Weiss Mail Stop 6-2 Mr. R. Kemp Mail Stop 6-2 Lewis Research Center Cleveland, OH 44135
1	Director NASA Scientific and Technical Information Facility ATTN: SAK/DL P.O. Box 8757 Baltimore/Washington International Airport, MD 21240
1	Director Lawrence Livermore Laboratory Technical Information Division P.O. Box 808 Livermore, CA 94550
1	Director Los Alamos Scientific Lab ATTN: Dr. J. Taylor P.O. Box 1663 Los Alamos, NM 87544
6	Sandia Laboratories ATTN: Infor Distr Division Dr. W. Herrmann Dr. S. W. Key Mr. R. D. Krieg Dr. A. Chabai Dr. W. A. von Riesemann Albuquerque, NM 87115
1	Director ATTN: J. Nall P.O. Box 1925 Washington, DC 20505
1	National Academy of Sciences ATTN: Mr. D. G. Groves 2101 Constitution Avenue, NW Washington, DC 20418
1	Aeronautical Research Associates of Princeton, Inc. ATTN: Dr. C. Donaldson 20 Washington Road Princeton, NJ 08540
1	Aerospace Corporation ATTN: Dr. Harris Mayer P.O. Box 95085 Los Angeles, CA 90045
2	AVCO Corporation Structures and Mechanics Dept ATTN: Dr. William Broding Mr. J. Gilmore Wilmington, MA 01887
2	Bell Aerosystems Company ATTN: Dr. W. H. Dukes Mr. J. Padlog P.O. Box 1 Buffalo, NY 14205
1	Bell Telephone Laboratories, Inc. ATTN: Mr. M. F. Stevens Mountain Avenue Murray Hill, NJ 07971
2	The Boeing Company Aerospace Group ATTN: Dr. Peter Grafton Dr. D. Strome Mail Stop 8C-68 Seattle, WA 98124
1	J. G. Engineering Research Associates 3831 Menlo Drive Baltimore, MD 21215

DISTRIBUTION LIST

No. of Copies	Organization
2	Kaman AviDyne ATTN: Dr. N. P. Hobbs Mr. S. Criscione Northwest Industrial Park 83 Second Avenue Burlington, MA 01803
3	Kaman Sciences Corporation ATTN: Dr. F. H. Shelton Dr. D. Sachs Dr. R. Keefe 1500 Garden of the Gods Road Colorado Springs, CO 80907
1	Knolls Atomic Power Lab ATTN: Dr. R. A. Powell Schenectady, NY 12309
2	Lockheed Missiles and Space Company, Inc. Division of Lockheed Aircraft Corporation ATTN: R. Robertson C. Vivian P.O. Box 504 Sunnyvale, CA 94088
3	Lockheed Missiles and Space Company Aerospace Research Laboratory ATTN: Dr. Bushnell Dr. R. Hartung Mr. P. Underwood 3251 Hanover Street Palo Alto, CA 94301
1	Martin Marietta Laboratories ATTN: Mr. R. Goldman 1450 S. Rolling Road Baltimore, MD 21227
1	Martin Marietta Laboratories ATTN: Mr. J. I. Bacile Orlando, FL 32805
1	McDonnell Douglas Astronautics Western Division ATTN: Mr. Samuel D. Mihara 3000 Ocean Park Boulevard Santa Monica, CA 90406
1	Physics International ATTN: Dr. G. Richard Fowles San Leandro, CA 94577
1	R&D Associates ATTN: Dr. Albert L. Latter P.O. Box 9695 Marina del Rey, CA 90291
1	Systems, Science and Software ATTN: Dr. J. K. Dienes P.O. Box 1620 La Jolla, CA 92037
2	Battelle Columbus Laboratories ATTN: Dr. L. E. Hulbert Mr. J. E. Backofen, Jr. 505 King Avenue Columbus, OH 43201
1	Brown University Division of Engineering ATTN: Prof R. Clifton Providence, RI 01912
1	Massachusetts Institute of Technology Aeroelastic and Structures Research Laboratory ATTN: Dr. E. A. Witmer Cambridge, MA 02139
1	Massachusetts Institute of Technology Department of Ocean Engineering ATTN: Prof Norman Jones Cambridge, MA 02139

DISTRIBUTION LIST

No. of Copies	Organization
1	Ohio State University Department of Engineering Mechanics ATTN: Prof K. K. Stevens Columbus, OH 43210
3	Southwest Research Institute ATTN: Dr. H. N. Abramson Dr. W. E. Baker Dr. U. S. Lindholm 8500 Culebra Road San Antonio, TX 78228
1	Stanford Research Institute ATTN: Dr. W. Reuland 306 Wynn Drive, NW Huntsville, AL 35805
1	Stanford University Department of Aeronautics and Astronautics ATTN: Prof C. R. Steele Stanford, CA 94305
1	Texas A & M University Department of Aerospace Engineering ATTN: Dr. Walter Haisler College Station, TX 77843
1	University of Alabama ATTN: Dr. T. L. Cost P.O. Box 2908 University, AL 35486
1	University of Delaware Department of Mechanical and Aerospace Engineering ATTN: Prof J. R. Vinson Newark, DE 19711
1	The City College of the University of New York Department of Mechanical Engineering ATTN: Prof S. B. Menkes New York, NY 10031

Aberdeen Proving Ground

Marine Corps Ln Ofc
Dir, USAMSAA
ATTN: Dr. J. Sperrazza
Mr. R. Norman, GWD